PROCEEDINGS

ENGINEERING WORKSHOP
ON
PEAK REDUCTION
FOR DRAINAGE AND FLOOD CONTROL PROJECTS

MAY 9, 1987

Sponsored by

AMERICAN SOCIETY OF CIVIL ENGINEERS

LOS ANGELES SECTION, ORANGE COUNTY BRANCH

■■■

DEPARTMENT OF CIVIL ENGINEERING

CALIFORNIA STATE UNIVERSITY, LONG BEACH

■■■

AMERICAN SOCIETY OF CIVIL ENGINEERS

STUDENT CHAPTER

CALIFORNIA STATE UNIVERSITY, LONG BEACH

INCLUDING UNCERTAINTY IN THE DESIGN OF FLOOD CONTROL PEAK REDUCTION SYSTEMS

T. V. Hromadka II, M.ASCE[1]

ABSTRACT: The classic single area unit hydrograph (UH) approach is widely used to model runoff response from a free draining catchment. Because the UH method correlates the effective rainfall distribution to the runoff hydrograph distribution, the resulting catchment UH should be considered a correlation distribution in a probabilistic sense. Should the uncertainty in rainfall over the catchment be a major concern in modeling reliability, then the UH output in the predictive setting must be considered to be a random variable. A case study demonstrates the procedure for including uncertainty in any peak flow reduction system.

INTRODUCTION

Many hydrologic models allow for the subdivision of the catchment into subareas, each linked by channel routing submodels (i.e., a link-node model). The effect of subdividing a catchment on modeling accuracy has not been fully investigated. The calibration of a link-node model to available rainfall-runoff data is a related issue, and the method of selecting the model parameters is important to the accuracy of the link-node modeling approach. Also, the uncertainty in the modeling boundary conditiions (i.e., the true precipitation distribution over the catchment) is propogated into the fitted parameters of the model itself, and the effect of insufficient knowledge of storm morphology affects model accuracy. These three factors (i.e., watershed subdivision, parameter estimation, and storm morphology effects) are important to the accuracy of hydrologic designs.

In this paper, the unit hydrograph method (UH) is used to develop estimates of runoff modeling error in the frequently occurring cases where the uncertainty in the rainfall distribution over the catchment dominates all other sources of modeling uncertainty. Indeed, the uncertainty in the precipitation distribution appears to be a limiting factor in the successful development, calibration, and application of all surface runoff hydrologic models (e.g., Loague and Freeze, 1985; Beard and Chang, 1979; Schilling and Fuchs, 1986; Garen and Burges, 1981; Nash and Sutcliffe, 1970; Troutman, 1982).

Schilling and Fuchs (1986) write "that the spatial resolution of rain data input is of paramount importance to the accuracy of the simulated hydrograph" due to "the high spatial variability of storms" and "the amplification of rainfall sampling

---

1 Director of Water Resources Engineering, Williamson and Schmid, Irvine, California and Research Associate, Princeton University, New Jersey

errors by the nonlinear transformation" of rainfall into runoff. They recommend that a model should employ a simplified surface flow model if there are many sub-basins; a simple runoff coefficient loss rate; and a diffusion (zero inertia) or storage channel routing technique.

In their study, Schilling and Fuchs (1986) reduced the rainfall data set resolution from a grid of 81 gages to a single catchment-centered gage in an 1,800 acre catchment. They noted that variations in runoff volumes and peak flows "are well above 100 percent over the entire range of storms implying that the spatial resolution of rainfall has a dominant influence on the reliability of computed runoff." It is also noted that "errors in the rainfall input are amplified by the rainfall-runoff transformation so that "a rainfall depth error of 30 percent results in a volume error of 60 percent and a peak flow error of 80 percent." They also write that "it is inappropriate to use a sophisticated runoff model to achieve a desired level of modeling accuracy if the spatial resolution of rain input is low" (in their study, the raingage densities considered for the 1,800-acre catchment are 81, 9, and a single centered gage).

Similarly, Beard and Chang (1979) write that in their study of 14 urban catchments, complex models such as continuous simulation typically have 20 to 40 parameters and functions that must be derived from recorded rainfall-runoff data. "Inasmuch as rainfall data are for scattered point locations and storm rainfall is highly variable in time and space, available data are generally inadequate for reliably calibrating the various interrelated functions of these complex models."

Garen and Burges (1981) noted the difficulties in rainfall measurement for use in the Stanford Watershed Model, because the K1 parameter (rainfall adjustment factor) and UZSN parameter (upper level storage) had the dominant impact on the model sensitivity.

In the extensive study by Loague and Freeze, (1985), three event-based rainfall-runoff models (a regression model, a unit hydrograph model, and a kinematic wave quasi-physically based model) were used on three data sets of 269 events from three small upland catchments. In that paper, the term "quasi-physically based", or QPB, is used for the kinematic wave model. The three catchments were 25 acres, 2.8 square miles, and 35 acres in size, and were extensively monitored with rain gage, stream gage, neutron probe, and soil parameter site testing. For example, the 25 acre site contained 35 neutron probe access sites, 26 soil parameter sites (all equally spaced), an on-site rain gage, and a stream gage. The QPB model utilized 22 overland flow planes and four channel segments. In comparative tests between the three modeling approaches to measured rainfall-runoff data it was concluded that all models performed poorly and that the QPB performance was only slightly improved by calibration of its most sensitive parameter, hydraulic conductivity. They write that the "conclusion one is forced to draw...is that the QPB model does not represent reality very well; in other words, there is considerable model error present. We suspect this is the case with most, if not all conceptual models currently in use." Additionally, "the fact that simpler, less data intensive models provided as good or better predictions than a QPB is food for thought."

Based on the literature, the main difficulty in the use, calibration, and development, of complex models appears to be the lack of precise rainfall data and the high model sensitivity to (and magnification of) rainfall measurements errors. Nash and Sutcliffe(1970) write that "As there is little point in applying exact laws to approximate boundary conditions, this, and the limited ranges of the variables encountered, suggest the use of simplified empirical relations."

Troutman (1982) also discusses the often cited difficulties with the error in precipitation measurements "due to the spatial variability of precipitation." This source of error can result in "serious errors in runoff prediction and large biases in parameter estimates by calibration of the model."

While surface runoff hydrologic models continue to be developed in technical component complexity, typically including additional algorithms for hydraulic routing effects and continuous soil moisture accounting, the problem setting continues to be poorly posed in a mathematical approximation sense in that the problem boundary conditions (i.e., the storm rainfall over the catchment) remain unknown. Indeed, the usual case in studying catchment runoff response is to have only a single rain gage and stream gage available for data analysis purposes; and oftentimes, neither gage is within the study catchment. As a result, the rainfall distribution over the catchment remains unknown; hence, the problem's boundary conditions must be approximated as part of the problem solution. The fact that the uncertainty in the rainfall distribution over the catchment has a major impact on the success of any hydrologic model's performance and accuracy (e.g., Schilling and Fuchs, 1986, and Troutman, 1982) indicates that the underlying assumption used to specify the storm rainfall over the catchment must necessarily be a major factor in the development, calibration, and application, of any hydrologic model.

CATCHMENT AND DATA DESCRIPTION

Let R be a free draining catchment with negligible detention effects. R is discretized into m subareas, R_j, each draining to a nodal point which is drained by a channel system. The m-subarea link node model resulting by combining the subarea runoffs for storm i, adding runoff hydrographs at nodal points, and routing through the channel system, is denoted as $Q_m^i(t)$. It is assumed that there is only a single rain gage and stream gage available for data analysis. The rain gage site is monitored for the 'true' effective rainfall distribution, $e_g^i(t)$. The motivation in using a measured $e_g^i(t)$ at the rain gage site is to avoid the necessity of using a multiparameter submodel to approximate $e_g^i(t)$; rather we assume that an accurate value of $e_g^i(t)$ is available, even though this data is measured at the rain gage site which may be located outside of the catchment. The stream gage data represents the entire catchment, R, and is denoted by $Q_g^i(t)$ for storm event i.

LINEAR EFFECTIVE RAINFALLS FOR SUBAREAS

The effective rainfall distribution (rainfall less losses) in R_j is given by $e_j^i(t)$ for storm i where $e_j^i(t)$ is assumed to be linear in $e_g^i(t)$ by:

$$e_j^i(t) = \sum \lambda_{jk}^i \, e_g^i(t - \theta_{jk}^i), \quad j = 1,2,\cdots,m \tag{1}$$

where λ_{jk}^i and θ_{jk}^i are coefficients and timing offsets, respectively, for storm i and subarea R_j. In Eq. (1), the variations in the effective rainfall distribution over R due to magnitude and timing are accounted for by the λ_{jk}^i and θ_{jk}^i, respectively. As an alternative to Eq. (1), the $e_g^i(t)$ may be defined as a set of unit effective rainfalls, each unit associated with its own proportion factor; however for simplicity, the use of the entire $e_g^i(t)$ function will be carried forward in the model development. Figure 1 illustrates the linear effective rainfall corresponding to arbitrary subarea, R_j.

SUBAREA RUNOFF

The storm i subarea runoff from R_j, $q_j^i(t)$, is given by the linear convolution integral:

$$q_j^i(t) = \int_{s=0}^{t} e_j^i(t - s)\, \phi_j^i(s)\, ds \qquad (2)$$

where $\phi_j^i(s)$ is the subarea unit hydrograph (UH) for storm i such that Eq. (2) applies. Combining Eqs. (1) and (2) gives

$$q_j^i(t) = \int_{s=0}^{t} \sum e_g^i(t - \theta_{jk}^i - s)\, \lambda_{jk}^i\, \phi_j^i(s)\, ds \qquad (3)$$

Rearranging variables,

$$q_j^i(t) = \int_{s=0}^{t} e_g^i(t - s) \sum \lambda_{jk}^i\, \phi_j^i(s - \theta_{jk}^i)\, ds \qquad (4)$$

where throughout this paper, the argument of the arbitrary frunction $F(s - Z)$ is notation that $F(s - Z) = 0$ for $s < Z$.

APPLICATION

To illustrate the linear effective rainfall concept, a simple model will be developed for the severe storm of March 1, 1983 over the 25 square mile Compton catchment in Los Angeles, California. This catchment is fully urbanized and is served by a well designed storm drain system which would have only minor backwater effects for the subject storm. The catchment has available a single rain gage and stream gage. The U.S. Army Corps of Engineers (Los Angeles District Office) or COE previously developed regionalized unit hydrographs for this area and, consequently, synthetic unit hydrographs can be estimated from the catchment characteristics of slope and other physical factors.

For demonstration purposes, the two-subarea model of Compton is used where the upstream subarea, R_1, runoff is modeled to be routed by pure translation (without peak flow attenuation) to the Compton stream gage where the second subarea, R_2, runoff is directly summed. For the above assumptions, the two-subarea model for storm event i is given by $Q_2^i(t)$ where

$$Q_2^i(t) = q_1^i(t - \tau_1^i) + q_2^i(t) \qquad (5)$$

where $q_1^i(t - \tau_1^i)$ is the $q_1^i(t)$ runoff from R_1 for storm i, offset in time by τ_1^i due to translation routing; and $q_2^i(t)$ is the runoff from R_2. From Eqs. (1) and (2), $Q_2^i(t)$ is rewritten as

$$Q_2^i(t) = \int_{s=0}^{t} \sum \lambda_{1k}^i \, e_g^i(t - \theta_{1k}^i) \, \phi_1^i(s - \tau_1^i) \, ds + \int_{s=0}^{t} \sum \lambda_{2k}^i \, e_g^i(t - \theta_{2k}^i) \, \phi_2^i(s) \, ds \quad (6)$$

The subarea UH's, $\phi_1(s)$ and $\phi_2(s)$ are estimated using the COE regionalized data. The appropriate sum of subarea runoffs, $q_1^i(t)$ and $Q_2^i(t)$, are then set equal to the stream gage for the storm, $Q_g^i(t)$, and the respective parameters λ_{jk}^i and θ_{jk}^i are estimated by minimizing the least-squares error, E, where

$$E = ||\omega_1 Q_g^i(t) - q_1^i(t - \tau_1^i)||_2 + ||\omega_2 Q_g^i(t) - q_2^i(t)||_2 \quad (7)$$

In Eq. (7), ω_1 and ω_2 are proportion factors defined by $\omega_1 = A_1/(A_1 + A_2)$ and $\omega_2 = A_2/(A_1 + A_2)$, where A_1, A_2 are the areas of R_1, R_2, respectively. Additionally, E is minimized with the constraint that all factors λ_{jk}^i are nonnegative. The timing offsets, θ_{jk}^i, used in Eq. (6) for this example are 15-minute offsets for the entire 24-hour storm duration. Thus, there are 96 translates being used to minimize E, for each subarea.

The resulting estimates for $e_j^i(t)$ are shown in Figs. 2a,b for subareas R_1 and R_2, respectively. Shown in the figures are the approximations of the $e_j^i(t)$ in comparison to the measured rain gage data, $P_g^i(t)$. From the figures it is seen that the estimated $e_j^i(t)$ are quite feasible as being the 'true' average effective rainfall distributions over R_1 and R_2. Figure 3 shows the comparison between the modeled $Q_2^i(t)$ results (using the $e_j^i(t)$ from Eq. (7)) and the stream gage data, $Q_g^i(t)$, for the subject storm.

Obviously, a different set of UH's in Eq. (6) will result in different $e_j^i(t)$ estimates in Eq. (7). However, the main objective of this simple application is only to demonstrate the feasibility and utility of the linear effective rainfall relationship of Eq. (1).

Each subarea's effective rainfall distribution, $e_j^i(t)$, can only be accurately determined by the use of runoff data from each subarea used in the model. Should subarea R_j have a stream gage to measure $e_j^i(t)$, then $e_j^i(t)$ can be equated to the "available" rain gage site measured effective rainfall, $e_g^i(t)$, by means of Eq. (1). For example, should subarea R_j experience zero rainfall during storm event i, the λ_{jk} in Eq. (1) would all be zero. Equation (1) provides a means to correlate the subarea R_j runoff for storm i, $q_j^i(t)$, to the available effective rainfall data measured at the rain gage site, $e_g^i(t)$.

It is noted that in the application problem, the λ_{jk}^i were optimized in Eq. (7) such that nonnegative values resulted. This constraint is used for the preference of avoiding negative runoff hydrographs which would result in the UH convolution process. Additionally, the use of the ω_1 and ω_2 factors in Eq. (7) based on the subarea arial proportions is used to facilitate the approximation effort.

LINEAR ROUTING

Let $I_1(t)$ be the inflow hydrograph to a channel flow routing link (number 1), and $Q_1(t)$ the outflow hydrograph. A linear routing model of the unsteady flow routing process is given by

$$Q_1(t) = \sum_{k_1=1}^{n_1} a_{k_1} I_1(t - \alpha_{k_1}) \tag{8}$$

where the a_{k_1} are coefficients which sum to unity; and the α_{k_1} are timing offsets. Again, $I_1(t-\alpha_{k_1}) = 0$ for $t < \alpha_{k_1}$. Given stream gage data for $I_1(t)$ and $Q_1(t)$, the best fit values for the a_{k_1} and α_{k_1} can be determined.

Should the above outflow hydrograph, $Q_1(t)$, now be routed through another link (number 2), then $I_2(t) = Q_1(t)$ and from the above

$$\begin{aligned} Q_2(t) &= \sum_{k_2=1}^{n_2} a_{k_2} I_2(t - \alpha_{k_2}) \\ &= \sum_{k_2=1}^{n_2} a_{k_2} \sum_{k_1=1}^{n_1} a_{k_1} I_1(t - \alpha_{k_1} - \alpha_{k_2}) \end{aligned} \tag{9}$$

For L links, each with their own respective stream gage routing data, the above linear routing technique results in the outflow hydrograph for link number L, $Q_L(t)$, being given by

$$Q_L(t) = \sum_{k_L=1}^{n_L} a_{k_L} \sum_{k_{L-1}=1}^{n_{L-1}} a_{k_{L-1}} \cdots \sum_{k_2=1}^{n_2} a_{k_2} \sum_{k_1=1}^{n_1} a_{k_1} I_1(t-\alpha_{k_1}-\alpha_{k_2}-\cdots-\alpha_{k_{L-1}}-\alpha_{k_L}) \tag{10}$$

Using the vector notation, the above $Q_L(t)$ is written as

$$Q_L(t) = \sum_{<k>} a_{<k>} I_1(t - \alpha_{<k>}) \tag{11}$$

For subarea R_j, the runoff hydrograph for storm i, $q_j^i(t)$, flows through L_j links before arriving at the stream gage and contributing to the total measured runoff hydrograph, $Q_g^i(t)$. All of the constants $a^i_{<k>}$ and $\alpha^i_{<k>}$ are available on a storm by storm basis. Consequently from the linearity of the routing technique, the m-subarea link node model is given by the sum of the m, $q_j^i(t)$ contributions,

$$Q_m^i(t) = \sum_{j=1}^{m} \sum_{<k>_j} a^i_{<k>_j} q_j^i(t - \alpha^i_{<k>}) \tag{12}$$

where each vector $\langle k \rangle_j$ is associated to a R_j, and all data is defined for storm i. It is noted that in all cases,

$$\sum_{\langle k \rangle_j} a^i_{\langle k \rangle_j} = 1 \tag{13}$$

APPLICATION

The linear routing technique of Eq. (8) is a variant of the stream flow routing convolution technique of Doyle et al (1983). For channel reach #1 (link #1), the linear routing parameters of proportions, a_{k_1}, and timing offets, α_{k_1}, can only be accurately determined by use of stream gage data which precisely give both the $I_1(t)$ and $O_1(t)$ used in Eq. (8).

Fortunately, the derived parameters from Eq. (8) provide good approximations for channel routing effects (without significant backwater effects) for a range of flow hydrographs. Hence for a class of hydrographs of similar magnitude, a single set of routing parameters may be appropriate with the linear routing model. Similarly, another class of hydrographs would have another associated set of calibrated routing parameters (e.g., Doyle et al, 1983). Hence, the linear routing technique is actual quasilinear in that the method is linear for specific ranges of runoff hydrographs.

To demonstreate the utility of the linear routing technique, a set of four hydrographs are considered in a channel reach of 10,000-foot length. All four hydrographs are routed through a prismatic channel using a fully-dynamic model solution as the 'true' solution. Using one hydrograph (Fig. 4), the model of Eq. (8) is calibrated. In this example, a least-squares error norm is used with the constraint that all proportions, a_{k_1}, are nonnegative. Only four timing offsets, α_{k_1}, were used in this application. The resulting calibration approximation and the 'exact' solution is shown in Fig. 4 for a fast flow (peak flow rate velocity of 24 feet/sec) and also a slow flow channel condition (peak flow rate velocity of 12 feet/sec). Using both sets of calibration parameters, four other hydrographs are tested and compared to the 'exact' solution in Fig. 5 for both the fast flow and slow flow conditions. From Fig. 5 it is seen that the linear routing method provides a good approximation of both translation and storage effects for a useful range of hydrograph magnitudes, even though only four timing offsets were used in the approximation effort.

This application not only illustrate the utility of the linear routing technique but also demonstrates that a calibrated linear routing model is also a good model for a range of hydrograph magnitudes. As noted in Doyle et al (1983), different sets of calibration parameters would be needed for different classes of hydrographs (e.g., low-flow hydrographs versus high-flows). However for specified range of classes of hydrographs, a single set of routing parameters may be appropriate. Hence, on a hydrograph class basis, the routing effects are essentially linear and are adequately described by the model of Eq. (8).

The above conclusions (i.e., that the routing effects are approximately linear for classes of hydrographs, and that a single set of calibrated routing parameters are appropriate for a class of hydrographs) will be useful in the latter sections of this paper when developing uncertainty estimates for hydrologic models.

LINK-NODE MODEL, $Q_m^i(t)$

For the above linear approximations for storm i, Eqs. (1), (4), and (12) can be combined to give the final form for the m subarea link-node model, $Q_m^i(t)$.

$$Q_m^i(t) = \sum_{j=1}^{m} \sum_{<k>_j} a^i_{<k>_j} \int_{s=0}^{t} e_g^i(t-s) \sum \lambda^i_{jk} \phi_j^i(s - \theta^i_{jk} - \alpha^i_{<k>_j}) \, ds \qquad (14)$$

Because the measured effective rainfall distribution, $e_g^i(t)$, is independent of the several indices, Eq. (14) is rewritten in the form

$$Q_m^i(t) = \int_{s=0}^{t} e_g^i(t-s) \sum_{j=1}^{m} \sum_{<k>} a^i_{<k>_j} \sum \lambda^i_{jk} \phi_j^i(s - \theta^i_{jk} - \alpha^i_{<k>_j}) \, ds \qquad (15)$$

where all parameters are evaluated on a storm by storm basis, i.

Equation (12) described a model which represents the total catchment runoff response based on variable subarea UH's, $\phi_j^i(s)$; variable effective rainfall distributions on a subarea-by-subarea basis with differences in magnitude (λ^i_{jk}), timing (θ^i_{jk}), and pattern shape (linearly assumption); and channel flow routing translation and storage effects (parameters $a^i_{<k>_j}$ and $\alpha^i_{<k>_j}$). All parameters employed in Eq. (15) must be evaluated by runoff data where stream gages are supplied to measure runoff from each subarea, R_j, and stream gages are located upstream and downstream of each channel reach (link) used in the model.

MODEL REDUCTION

The m-subarea model of Eq. (15) is directly reudced to the simple single area UH model (no discretization of R into subareas) given by $Q_1^i(t)$ where

$$Q_1^i(t) = \int_{s=0}^{t} e_g^i(t-s) \, \eta^i(s) \, ds \qquad (16)$$

where $\eta^i(s)$ is the correlation distribution between the data pair $\{Q_g^i(t), e_g^i(t)\}$, for storm event i.

From Eq. (16) it is seen that the classic single area UH model equates to the highly complex link node modeling structure of Eq. (15), where considerable runoff gage data is supplied interior to the catchment, R, so that all modeling parameters are accurately calibrated on a storm-by-storm basis. For the case of having available only a single rain gage site (where the effective rainfall is measured, $e_g^1(t)$) and a stream gage for data correlation purposes, the $\eta^1(s)$ properly represents the several effects used in the development leading to Eq. (15), integrated according to the observed sampling from the several modeling parameters' respective probability distributions. Because the simple $Q_1^1(t)$ model structure actually includes most of the effects which are important in flood control hydrologic response, it can be used to develop useful probabilistic distributions of hydrologic modeling output.

In comparing the two models of Eqs. (15) and (16), it is noted that $Q_m^i(t) = Q_1^i(t)$ only when interior runoff data is supplied to accurately evaluate all the modeling parameters used in Eq. (15). For example, should the catchment be discretized into many small subareas with small channel routing links (e.g., such as used in highly subdivided catchments with UH approximations, or as employed in kinematic wave (Kw) type models such as MITCAT, or the KW version of HEC-1), then with a stream gage located at each subarea (or overland flowplane) and at each channel link, all modeling parameters could be accurately evaluated on a storm-by-storm basis, resulting in the formulation of Eq. (15).

Indeed, only by means of subarea stream gage data can the subarea linear effective rainfall distribution parameters of λ_{jk}^i and θ_{jk}^i be accurately determined for each storm event i. But it is these linear effective rainfall distribution parameters that reflect the important spatial and temporal variability of storm rainfall over the catchment which in turn causes the major difficulties in the development, calibration, and use, of hydrologic models (Schilling and Fuchs, 1986; Troutman, 1983; among others).

It is assumed in this paper that only a single rain gage (which is monitored to accurately develop the effective rainfall at the rain gage site, $e_g^i(t)$) and stream gage are available for data analysis. Consequently, any hydrologic model serves to correlate the data pair $\{e_g^i(t), Q_g^i(t)\}$ for each storm event i.

The current direction of advanced development for hydrologic models is a modeling structure such as Eq. (15). With subarea and channel-link stream gage data, the $Q_m^i(t)$ parameters can be accurately determined, and

$$Q_m^i(t) = Q_1^i(t) \tag{17a}$$

But in the typical case of having only the single rain gage and stream gage, all the parameters in Eq. (15) must be approximated, resulting in the estimator, $\hat{Q}_m^i(t)$, wherein the subarea linear effective rainfall parameters of Eq. (1) are misrepresented by setting $\theta_{jk}^i = 0$ (i.e., zero timing offsets between the measured rainfall at the gage and the subarea rainfalls), and also by assuming that the magnitudes of rainfall intensities are invariant between subareas and the rain gage.

From the above discussion, the estimator model, $\hat{Q}_m^i(t)$, cannot achieve the accuracy of $Q_m^i(t)$, (and hence, $Q_1^i(t)$):

$$\hat{Q}_m^i(t) \neq Q_m^i(t) \tag{17b}$$

and from Eq. (17),

$$\hat{Q}_m^i(t) \neq Q_1^i(t) \tag{17c}$$

From Eqs. (17), the simple single area UH model, $Q_1^i(t)$, properly represents the appropriate UH for each subarea (or overland flow plane) for storm i; the appropriate linear routing parameters for each channel link, for storm i; the appropriate timing offsets and proportions of the measured effective rainfalls, for each subarea; and the appropriate summation of runoff hydrographs at each confluence. In contrast, the model estimator, $\hat{Q}_m^i(t)$, uses estimates for all of the parameters, and subarea effective rainfall factors, and hence cannot achieve the accuracy of $Q_1^i(t)$ without the

addition of interior rainfall-runoff data to accurately validate the parameter values.

STORM CLASSIFICATION SYSTEM

To proceed with the analysis, the full domain of effective rainfall distributions measured at the rain gage site are categorized into storm classes, $\langle \xi_x \rangle$. Because the storm classifications are based upon effective rainfalls, the measured precipitations, $P_g^i(t)$, may vary considerably yet produce similar effective rainfall distributions. That is, any two elements of a class $\langle \xi_x \rangle$ would result in nearly identical effective rainfall distributions at the rain gage site, and hence one would "expect" nearly identical runoff hydrographs recorded at the stream gage. Typically, however, the resulting runoff hydrographs differ and, therefore, the randomness of the effective rainfall distribution over the catchment, R, results in variations in the modeling "best-fit" parameters (i.e., in $Q_1^i(t)$, the $\eta^i(s)$ variations) in correlating the available rainfall-runoff data.

More precisely, any element of a specific storm class $\langle \xi_o \rangle$ has the effective rainfall distribution, $e_g^o(t)$. However, there are several runoffs associated to the single $e_g^o(t)$, and are noted by $Q_g^{oi}(t)$. In correlating $\{Q_g^{oi}(t), e_g^o(t)\}$, a different $\eta^i(s)$ results due to the variations in the measured $Q_g^{oi}(t)$ with respect to the single known input at the rain gage site, $e_g^o(t)$.

In the predictive mode, where one is given an assumed (or design) effective rainfall distribution, $e_g^D(t)$, to apply at the rain gage site, the storm class of which $e_g^D(t)$ is an element of is identified, $\langle \xi_D \rangle$, and the predictive output for the input, $e_g^D(t)$, must necessarily be the random variable or distribution,

$$[Q_1^D(t)] = \int_{s=0}^{t} e_g^D(t - s)\, [\eta(s)]_D \, ds \qquad (18)$$

where $[\eta(s)]_D$ is the distribution of $\eta^i(s)$ distributions associated to storm class $[\xi_D]$.

Generally, however, there is insufficient rainfall-runoff data to derive a statistically significant set of storm classes, $\langle \xi_x \rangle$, and hence additional assumptions must be used. For example, one may lower the eligibility standards for each storm class, $\langle \xi_x \rangle$, implicitly assuming that several distributions $[\eta(s)]_x$ are nearly identical; or one may transfer $[\eta(s)]_x$ distributions from another rainfall-runoff data set, implicitly assuming that the two catchment data set correlation distribution are nearly identical. A common occurrence is the case of predicting the runoff response from a design storm effective rainfall distribution, $e_g^D(t)$, which is not an element of any observed storm class. In this case, another storm class distribution must be used, which implicitly assumes that the two sets of correlation distributions are nearly identical. Consequently for a severe design storm condition, it would be preferable to develop correlation distributions using the severe historic storms which have rainfall-runoff data available for the appropriate condition of the catchment.

EFFECTIVE RAINFALL UNCERTAINTY AND THE DISTRIBUTIONS, $[\eta(s)]_x$

This paper's introduction includes brief statements from several reports which conclude that the variability in the rainfall (and hence the effective rainfall) over the catchment is a dominant factor in the development, calibration, and application, of hydrologic models (e.g., Schilling and Fuchs, 1986; among others).

Including this premise in hydrologic studies would indicate that hydrologic model estimates must be functions of random variables, and hence the estimates are random variables themselves.

From Eq. (15), the correlation distribution for storm event i, $\eta^i(s)$, includes all the uncertainty in the effective rainfall distribution over R, as well as the uncertainty in the runoff and flow routing processes. That is, $\eta^i(s)$ must be an element of the random variable $[\eta(s)]_x$ where

$$\eta^i(s) = \sum_{j=1}^{m} \sum_{<k>_j} a^i_{<k>_j} \sum \lambda^i_{jk} \phi_j{}^i(s - \theta^i_{jk} - \alpha^i_{<k>_j}) \qquad (19)$$

and Eq. (19) applies to storm event i for some storm class $<\xi_x>$. For severe storms of flood control interest, one would be dealing with only a subset of the set of all storm classes. In a particular storm class, $<\xi_o>$, should it be assumed that the subarea runoff parameters and channel flow routing uncertainties are minor in comparison to the uncertainties in the effective rainfall distribution over R (e.g., Schilling and Fuchs, 1986; among others), then Eq. (15) may be written as

$$[\eta(s)]_o = \sum_{j=1}^{m} \sum_{<k>} \bar{a}_{<k>_j} \sum [\lambda_{jk}] \bar{\phi}_j \ (s - [\theta_{jk}] - \bar{\alpha}_{<k>_j}) \qquad (20)$$

where the overbars are notation for mean values of the parameters for storm class $<\xi_o>$. But the mean values for the linear routing parameters are essentially the calibrated parameters corresponding to a class of hydrographs (see the application following Eq. (13)) which accommodates a range of hydrograph magnitudes. And for a highly discretized catchment model, the use of a mean value UH for each subarea, $\phi_j(s)$, has only a minor influence in the total model results (Schilling and Fuchs, 1986). Although use of Eq. (16) in deriving the $[\eta(s)]_o$ distributions results in the uncertainties of both the effective rainfalls and also the channel routing and other processes being integrated, Eq. (20) is useful in motivating the use of the probabilistic distribution concept in design and planning studies for all hydrologic models, based on just the magnitude of the uncertainties in the effective rainfall distribution over R. That is, although one may argue that a particular model is "physically based" and represents the "true" hydraulic response distributed throughout the catchment, the uncertainty in rainfall still remains and is not reduced by increasing hydraulic routing modeling complexity. Rather, the uncertainty in rainfall is reduced only the use of additional rainfall-runoff data. In Eq. (20), the use of mean value parameters for the routing effects implicitly assumes that the variations in storm parameters of $[\lambda_{jk}]$ $[\theta_{jk}]$ are not so large such as to develop runoff hydrographs which cannot be modeled by a single set of linear routing parameters on a channel link-by-link basis.

DISCRETIZATION ERROR

In the general case, the practitioner generally assigns the recorded precipitation from the single available rain gage, $P_g{}^i(t)$, to occur simultaneously over each subarea, R_j. That is from Eq. (1), the $\theta^i_{jk} \equiv 0$ and the λ^i_{jk} are set to constants $\hat{\lambda}_j$ which reflect only the variations in loss rate nonhomogeneity. Hence, the 'true' $Q_m{}^i(t)$ model of Eq. (15), (and also Eq. (16)), becomes the estimator $\hat{Q}_m{}^i(t)$ where

$$\hat{Q}_m^{\,i}(t) = \int_{s=0}^{t} \hat{e}_g^{\,i}(t-s) \sum_{j=1}^{m} \sum_{<k>} \hat{a}_{<k>_j} \sum \hat{\lambda}_j \hat{\phi}_j^{\,i}(s - \hat{\alpha}^i_{<k>_j})\, ds \qquad (21)$$

where hats are notation for estimates. These incorrect assumptions result in 'discretization error'. Indeed, an obvious example of discretization error is the case where a subarea R_j actually receives no rainfall, and yet one assumes that $P_g^{\,1}(t)$ occurs over R_j in the discretized model. (It is easily shown that the Eq. (16) model accommodates this example case.)

DISCRETIZATION CALIBRATION ERROR

A current trend among practitioners is to develop an m-subarea link-node model estimator $\hat{Q}_m^{\,i}(t)$ such as Eq. (21), and then "calibrate" the model parameters using the available (single) rain gage and stream gage data pair. Because subarea rainfall-runoff data are unavailable, necessarily it is assumed that the random variables associated to the subarea effective rainfalls are given by

$$\left.\begin{aligned} [\theta_{jk}] &= 0 \\ [\lambda_{jk}] &= \hat{\lambda}_j \end{aligned}\right\} \text{ (estimator, } \hat{Q}_m^{\,i}(t), \text{ assumptions)} \qquad (22)$$

But these assumptions violate the previously stated premise that the uncertainty in the effective rainfall distribution over R has a major effect in hydrologic modeling accuracy. The impact in using Eq. (22) becomes apparent when calibrating the model to only storms of a single storm class, $<\xi_o>$.

Again, for all storms in $<\xi_o>$, the effective rainfall distributions are all nearly identical and are given by the single input, $e_g^{\,o}(t)$. But due to the variability in rainfall across the R_j, the associated runoff hydrographs, $Q_g^{oi}(t)$, differ even though $e_g^{\,o}(t)$ is the single model input.

It is recalled that in Eq. (21), the effective rainfall distribution is now the estimator, $\hat{e}_g^{\,oi}(t)$. That is, due to the several assumptions leading to Eq. (22) for the discretized model estimator, $\hat{Q}_m^{\,i}(t)$, the variations due to $[\lambda_{jk}]$ and $[\theta_{jk}]$ are transferred from the $[\eta(s)]$ distribution to the $\hat{e}_g^{\,i}(t)$ function. For storm class $<\xi_o>$, the estimator $\hat{Q}_m^{\,oi}(t)$ can be written from Eqs. (20) and (21) as

$$\hat{Q}_m^{oi}(t) = \int_{s=0}^{t} \hat{e}_g^{oi}(t-s) \sum_{j=1}^{m} \sum_{<k>} \bar{a}_{<k>_j} \sum \hat{\lambda}_j \bar{\phi}_j(s - \bar{\alpha}_{<k>})\, ds \qquad (23)$$

where in Eq. (23), it is assumed that the variations in model output due to using mean values (overbar notation) are minor in comparison to the variations in model output due to $[\lambda_{jk}]$ and $[\theta_{jk}]$. That is, even though the rainfall distributions over the catchment, R, are variable with respect to the single input, $e_g^{oi}(t)$, the resulting subarea runoffs still fall within a single linear routing parameter class for each channel routing link, respectively. But then Eq. (23) is but another single area UH model:

$$\hat{Q}_m^{oi}(t) = \int_{s=0}^{t} \hat{e}_g^{oi}(t - s)\, \hat{\eta}_o(s)\, ds \qquad (24)$$

where $\hat{\eta}_o(s)$ is an estimated distribution which is 'fixed' for all storms in a specified storm class $<\xi_o>$. In calibrating $\hat{Q}_m^{oi}(t)$, therefore, the work effort is focused towards finding the best fit effective rainfall distribution $\hat{e}_g^{oi}(t)$, which correlates the data pairs $\{Q_g^i(t), \hat{\eta}_o(s)\}$, for each storm i. That is, the 'true' single $e_g^o(t)$ is modified to be $\hat{e}_g^{oi}(t)$ in order to correlate the $\{Q_g^{oi}(t), \hat{\eta}_o(s)\}$, for each storm i. This contrasts with finding the best fit $\eta^i(s)$ which correlates the pairs, $\{Q_g^{oi}(t), e_g^o(t)\}$, such as in Eq. (16). It is recalled that from Eqs. (20), (21), and (24), $\hat{\eta}_o(s)$ is a single distribution due to the assumptions of Eq. (22), and due to using a single storm class, $<\xi_o>$, which develops runoffs that fall within a single class of linear routing hydrographs.

The effective rainfall estimator, $\hat{e}_g^{oi}(t)$, used in Eqs. (23) and (24) is the correlation between the data pair $\{Q_g^{oi}(t), \hat{\eta}_o(s)\}$. Consequently, similar to the $\eta^i(s)$ distributions, the $\hat{e}_g^{oi}(t)$ must have an infinite degrees of freedom in order to provide the needed correlation. However, hydrologic models prescribe a given model structure to the effective rainfall estimator which involves only a finite number of degrees of freedom, or parameters. This fixed model structure develops effective rainfalls, noted as $\tilde{e}_g^i(t)$, for storm event i. Convoluting $\tilde{e}_g^i(t)$ with the $\hat{\eta}_o(s)$ estimated for storm class $<\xi_o>$ develops the general hydrologic model, $\tilde{Q}_g^i(t)$, for storm i. The model $\tilde{Q}_g^i(t)$ is the model that practictioners use. For storm class $<\xi_o>$, the correlation distribution is the fixed $\hat{\eta}_o(s)$, and the effective rainfall estimator is the single calibrated distribution $\tilde{e}_g^o(t)$. Thus, for storm class $<\xi_o>$, the 'true' hydrologic model structure of Eq. (15) becomes the point estimate:

$$\tilde{Q}_m^o(t) = \int_{s=0}^{t} \tilde{e}_g^o(t - s)\, \hat{\eta}_o(s)\, ds \qquad (25)$$

Because the effective rainfall submodel used in $\tilde{Q}_m^i(t)$ has a prescribed structure, it cannot match the best fit $\hat{e}_g^{oi}(t)$ for all storms and, consequently, modeling error is introduced into the parameters of the loss rate submodel, $\tilde{e}_g^o(t)$, when calibrated to storm class $<\xi_o>$.

An error which results due to use of Eq. (25) is that the estimator modeling distribution $[\tilde{Q}_m(t)]$ for storm class $<\xi_o>$ will be imprecise due to the variation in derived loss rate parameters in $\tilde{e}_g^o(t)$ not achieving the true variation in $\hat{e}_g^{oi}(t)$ needed to correlate $\{Q_g^{oi}(t), \hat{\eta}_o(s)\}$ in Eq. (24).

HYDROLOGIC MODEL OUTPUT DISTRIBUTIONS

The previous development resulted in the identification of four modeling structures:

(i) $Q_m^i(t)$ -- this is the m-subarea link node model with channel links connecting the subareas, (Eq. (15)). Stream gage data is supplied for each subarea (or overland flowplane) and also along each channel link so that all modeling parameters and subarea effective rainfall factors are accurately determined for each storm event i. For storm class $<\xi_o>$, (measured at the single

"available" rain gage site), $Q_m^i(t)$ results in the distribution, $[Q_m^o(t)]$.

(ii) $Q_1^i(t)$ -- this is a simple single area UH model. For only a single rain gage and stream gage, $Q_1^i(t)$ is equal to $Q_m^i(t)$ in predicting runoff at the stream gage (see Eqs. (15) and (16)). For storm class $<\xi_o>$, $Q_1^i(t)$ becomes the distribution $[Q_1^o(t)]$ where $[Q_1^o(t)] = [Q_m^o(t)]$.

(iii) $\hat{Q}_m^i(t)$ -- should all the parameters in $Q_m^i(t)$ be estimated for a storm class, then $Q_m^i(t)$ is approximated by the estimator $\hat{Q}_m^i(t)$. However on a storm class basis, $\hat{Q}_m^i(t)$ reduces to another single area UH model of Eq. (24) where the correlation distribution, $\hat{n}_o(s)$, is fixed for storm class $<\xi_o>$. $\hat{Q}_m^i(t)$ equates to $Q_m^i(t)$ when the effective rainfall estimator, $\hat{e}_g^i(t)$, is given an infinite number of degrees of freedom.

(iv) $\tilde{Q}_m^i(t)$ == because the effective rainfall estimates in an m-subarea link node model are of a prescribed structure, the estimates have a finite number of degrees of freedom. For storm class $<\xi_o>$, $\tilde{Q}_m^i(t)$ reduces to another single area UH model where the correlation distribution is identical to that used in $\hat{Q}_m^i(t)$. But the effective rainfall distritubion in the single area UH representation is $\tilde{e}_g^i(t)$ where $\tilde{e}_g^i(t)$ is calibrated to best fit the distribution of $\hat{e}_g^i(t)$ distributions which are needed to correlate the data pairs, $\{\hat{Q}_g^i(t), \hat{n}_o(s)\}$, in storm class $<\xi_o>$.

From the four modeling structures, the parameter calibration process can be interpretted. For storm class $<\xi_o>$, distributions are developed for $[Q_m^o(t)]$ and $[Q_1^o(t)]$. A distribution of $\hat{Q}_m^i(t)$, noted as $[\hat{Q}_m^o(t)]$, can be developed provided the effective rainfall estimator is given an infinite number of degrees of freedom. However, the "calibrated" model of $Q_m^i(t)$ develops only a single point estimate $\tilde{Q}_m^o(t)$ for storm class $<\xi_o>$.

For storm class $<\xi_o>$, the several modeling output distributions are as follows:

$$[Q_m^o(t)] = \int_{s=0}^{t} e_g^o(t-s) \sum_j \sum_{<k>} a^o{}_{<k>_j} \sum [\lambda_{jk}^o] \phi_j^o(s-[\theta_{jk}^o]-\alpha^o{}_{<k>_j}) \, ds \tag{26}$$

$$[Q_1^o(t)] = \int_{s=0}^{t} e_g^o(t-s) \, [n(s)]_o \, ds \tag{27}$$

$$[\hat{Q}_m^o(t)] = \int [\hat{e}_g^o(t-s)] \, \hat{n}_o(s) \, ds \tag{28}$$

$$[\tilde{Q}_m^o(t)] = \tilde{Q}_m^o(t) = \int_{s=0}^{t} \tilde{e}_g^o(t-s) \, \hat{n}_o(s) \, ds \tag{29}$$

Again, $[Q_m^o(t)] = [Q_1^o(t)]$. $[\hat{Q}_m^o(t)] = [Q_m^o(t)]$ only when $\hat{e}_g^{oi}(t)$ is given an infinite number of degrees of freedom such as to correlate $Q_g^{oi}(t)$ to $\hat{n}_o(s)$ for each storm i. Finally, $\tilde{e}_g^o(t)$ is some weighted average of the distribution of $[\hat{e}_g^o(t)]$, usually, the expected value is used:

$$\tilde{e}_g^o(t) = E[\hat{e}_g^o(t)] \tag{30}$$

APPLICATION: THE CALIBRATION PROCESS

In calibrating the model structure, $Q_1^i(t)$, for storm class $<\xi_o>$, the data $Q_g^{oi}(t)$ and $e_g^o(t)$ is used to determine the distribution of $[n(s)]_o$.

In calibrating the model structure, $\hat{Q}_m^i(t)$, the data $Q_g^{oi}(t)$ and the rigid $\hat{n}_o(s)$ is used to determine a best fit $\hat{e}_g^{oi}(t)$ for each storm i in class $<\xi_o>$.

In calibrating the model structure, $\tilde{Q}_m^i(t)$, the effective rainfall function, $\tilde{e}_g^o(t)$, is calibrated to best fit the distribution of $[\hat{e}_g^o(t)]$ such as by using a simple average.

To demonstrate the above discussion, a 25-subarea link-node model of an idealized catchment is used which satisfies the several assumptions leading to $Q_m^i(t)$, (see Fig. 6). The single "available" rain gage is shown as a triangle in Fig. 6. Not shown in Fig. 6 are subarea-centered rain gages and link stream gages which are used in $Q_m^1(t)$, but are "unavailable" to the estimator, $\hat{Q}_m^1(t)$. The catchment, R, is 1000 acres in size, with each R_j being 40 acres. All channel links are rectangular channels with dimensions of depth $\stackrel{\Delta}{=}$ 20-feet (so as to guarantee no overflow), width = 8-feet, slope = 0.01 ft/ft, and a Mannings friction factor of 0.015.

Each subarea has its own UH (standard SCS triangular unit hydrograph) which is assumed to be a function of its time of concentration, Tc. Each subarea is assumed to have a uniform loss rate function. The rain gage site is monitored to determine the 'true' effective rainfall, $e_g^1(t)$, (Fig. 6).

To evaluate the calibration process, a series of identical effective rainfall distributions (i.e., storms $e_g^o(t)$ are defined at the rain gage site, which satisfy that each storm is in the same storm class, $<\xi_o>$). For the model structure of $\hat{Q}_m^o(t)$, the subarea effective rainfalls are assumed related to the $e_g^o(t)$ by the factors $\hat{\lambda}_j$ listed in Table 1. Other parameter data is also listed in this table. The 'true' distributions of $e_j^{oi}(t)$ are random variables distributed according to Fig. 7a for λ_{jk}^{oi}, and Fig. 7b for timing offsets, θ_{jk}^{oi}, where mean values are listed in Table 1. The 'ture' runoff hydrographs are developed for each storm using $Q_m^1(t)$ of Eq. (15), and are shown in Fig. 8. The variations in runoff shown in Fig. 8 are of the order of magnitude reported in Schilling and Fuchs (1986), and should provide a useful case study in examining the model calibration process.

Because $e_g^o(t)$ is fixed, the $\hat{Q}_m^o(t)$ model structure must have a fixed output. Therefore, because $\hat{n}_o(s)$ is fixed, a least-squares best fit for $\hat{e}_g^{oi}(t)$ can be developed for each storm in $<\xi_o>$. Some of the resulting plots of effective rainfall distributions are shown in Fig. 9. In the figure, it is seen that a different $\hat{e}_g^{oi}(t)$ is derived for each storm i (in class $<\xi_o>$) in correlating $\{Q_g^{oi}(t), \hat{n}(s)\}$.

For $Q_1^{oi}(t)$, however, the variations in $e_j^{oi}(t)$ are reflected in the $n_o^i(s)$ variations. Some of the elements of the set $\{n_o^i(s)\}$ are shown in summation (mass) graph form in Fig. 10.

TABLE 1. APPLICATION PROBLEM DATA

Subarea R_j	Tc[1]	$\hat{\lambda}_j$[2]	$\bar{\lambda}^o_{jk}$[3]	$\bar{\theta}^o_{jk}$[4]
1	30	1	1	0
2	30	1	1	0
3	45	1	1	0
4	45	1.1	1.1	3
5	30	1.1	1.1	3
6	30	.9	.9	3
7	45	.8	.8	3
8	30	.8	.8	3
9	30	.7	.7	3
10	30	.7	.7	3
11	45	.8	.8	6
12	45	1.	1.	6
13	45	1.	1.	6
14	45	1.3	1.3	6
15	30	1.3	1.3	6
16	30	1.2	1.2	6
17	45	1.2	1.2	6
18	30	1.1	1.1	6
19	30	1.1	1.1	6
20	45	1.	1.	6
21	30	1.	1.	6
22	30	1.	1.	6
23	30	.9	.9	6
24	45	.9	.9	6
25	45	.8	.8	6

Notes:

1. Tc = time of concentration in minutes
2. $\hat{\lambda}_j$ = assumed ratio of effective rainfall at subarea to rain gage site
3. $\bar{\lambda}_{jk}$ = mean value for λ^i_{jk}. Note that $\bar{\lambda}_{jk} = \hat{\lambda}_j$
4. $\bar{\theta}_{jk}$ = mean value for θ^i_{jk}, in minutes

From Fig. 9, the set of $\hat{e}_g^{oi}(t)$ plots needed to correlate the $Q_g^{oi}(t)$ to the single $\hat{\eta}_o(s)$ cannot be duplicated by a fixed loss rate model structure because the storm precipitation is identical for each event and, therefore, a loss in accuracy must occur during parameter calibration. Additionally, the final calibrated parameters lose some of the physical meaning for what they were intended, in that they reflect variations in effects other than the loss rate. The model structure, $\tilde{Q}_m^{\,i}(t)$, uses a "calibrated" effective rainfall distribution, $\tilde{e}_g^{\,o}(t)$, which is usually an average of the derived $\hat{e}_g^{oi}(t)$; this is shown as the heavy line in Fig. 9. Whether $\tilde{e}_g^{\,o}(t)$ can fit the heavy line in Fig. 9 depends on the prescribed model structure of the loss function.

In Fig. 10, however, the resulting $\eta_o^{\,i}(s)$ plots (summation graph form) are used to populate a frequency distribution for $[\eta(s)]_o$ to develop the uncertainty distribution for $[Q_1^{\,o}(t)]$ using the single measured $e_g^{\,o}(t)$ as the model input.

It is noted that in this application, the estimated $\hat{\lambda}_j$ are assumed "correctly" in that the $\hat{\lambda}_j$ equal the mean value of λ_{jk} (see Table 1). Hence the actual applications, the discrepancies between $\hat{e}_g^{oi}(t)$ could be augmented.

DISCUSSION

The application demonstrates how the unknown effective rainfall distribution manifests itself in the single area UH, $Q_1^{\,i}(t)$, model, and in a discretized link node model estimator, $\tilde{Q}_m^{\,i}(t)$, when using storms of a similar class to calibrate model parameters. For the $Q_1^{\,i}(t)$ model, the uncertainties are incorporated into the UH correlation distribution, $\eta^i(s)$. In the estimator, $\tilde{Q}_m^{\,i}(t)$, however, the uncertainties are transferred to the effective rainfall submodel parameters used in $\tilde{e}_g^{\,i}(t)$.

Because the $\eta^i(s)$ are allowed to freely vary, the frequency distribution $[\eta(s)]_o$ of the $\eta^{oi}(s)$ reflect the several modeling uncertainties as well as the important uncertainty in the effective rainfall distribution over R, for storm class $\langle\xi_o\rangle$.

With the estimator, $\tilde{Q}_m^{\,i}(t)$, however, the effective rainfall estimator, $\tilde{e}_g^{\,i}(t)$, is a fixed model structure which cannot fit the irregular effective rainfall distributions needed to correlate measured runoff data, $Q_g^{oi}(t)$, to the $\tilde{Q}_m^{\,i}(t)$ model single UH correlation distribution, $\hat{\eta}_o(s)$, for storm class $\langle\xi_o\rangle$. As a result, the calibration of $\tilde{e}_g^{\,i}(t)$ must be imprecise and, therefore, the $\tilde{Q}_m^{\,i}(t)$ must be a more uncertain model in the predictive mode than the $Q_1^{\,i}(t)$ model on a storm class basis.

THE VARIANCE OF HYDROLOGIC MODEL OUTPUT

Consider the $Q_1^{\,i}(t)$ model structure in correlating the single rain gage and stream gage. For storm class $\langle\xi_o\rangle$, there is an associated distribution of correlation distributions, $[\eta(s)]_o$. Then in the predictive mode, the predicted hydrologic model output is the distribution $[Q_1^{\,o}(t)]$ where

$$[Q_1^{\,o}(t)] = \int_{s=0}^{t} e_g^{\,o}(t-s)\,[\eta(s)]_o\,ds \qquad \text{(from Eq. 26)}$$

For storm time z, the distribution of flow rate values is by $[Q_1^{\,o}(z)]$, where

$$[Q_1^{o}(z)] = \int_{s=0}^{t} e_g^{o}(z - s)\ [\eta(s)]_o\ ds \tag{31}$$

Let t_p be the storm time where the peak flow rate, Q_p, occurs for storm class $<\xi_o>$. Noting that t_p is a function of $[\eta(s)]_o$, then the distribution of $[Q_p]_o$ is given by

$$[Q_p]_o = \int_{s=0}^{t_p} e_g^{o}(t_p - s)\ [\eta(s)]_o\ ds \tag{32}$$

Let $\mathcal{D}$ be a single time duration. Of interest is the maximum volume of runoff during duration, $\mathcal{D}$, for storm class $<\xi_o>$. Then the distribution of this estimate is given by

$$[\max \int_{\mathcal{D}} Q_1^{o}(t)dt] = \max \int_{\mathcal{D}} \int_{s=0}^{t} e_g^{o}(t - s)[\eta(s)]_o\ ds \tag{33}$$

Let A be an operator which represents a hydrologic process algorithm (e.g., detention basin, etc.). Then the output of the operator for storm class $<\xi_o>$ is the distribution

$$[A]_o = A\left(\int_{s=0}^{t} e_g^{o}(t - s)\ [\eta(s)]_o\ ds \right) \tag{34}$$

The expected value of the hydrologic process A for storm class $<\xi_o>$ is

$$E[A]_o = \sum_{[\eta(s)]_o} A\left(\int_{s=0}^{t} e_g^{o}(t - s)\ \eta(s)\ ds \right) P(\eta(s)) \tag{35}$$

where $P(\eta(s))$ is the frequency of occurrance for distribution $\eta(s)$ in $[\eta(s)]_o$. The variance of predictions of hydrologic process A for storm class $<\xi_o>$ is (for A ( ) being a mapping into the real number line; i.e., giving a single number result),

$$var[A]_o = \sum_{[\eta(s)]_o} \left(A\left(\int_{s=0}^{t} e_g^{o}(t - s)\ \eta(s)\ ds \right) - E[A]_o \right)^2 P(\eta(s)) \tag{36}$$

From the above standard statistical definitions, and Eqs. (26)-(29), it is seen that the $\text{var}[A]_Q$ is computed correctly when the single area UH model structure distribution, $[Q_1^o(t)]$, is used for storm class $\langle \xi_o \rangle$. The use of additional subareas in the modeling structure (for the given assumptions) must be accompanied by runoff data in order to properly evaluate the effective rainfall distribution in each subarea with respect to the available single rain gage data site. Without this additional data, the variance in modeling output will not equate to the true variance provided by $[Q_1^o(t)]$ for storm class $\langle \xi_o \rangle$. Because the model estimator of Eq. (29) cannot produce design estimates more accurately than the single area UH model of Eq. (27), the variance of Eq. (36) must be a lower bound for all hydrologic models.

APPLICATIONS

Dominguez Wash is a fully develop 35 square-mile catchment located in Los Angeles, California. It has been essentially fully improved with a well-drained flood control system for nearly 50-years. Of concern is the design of a flood control detention basin at the stream gage site.

The design objective is to build a flow-through type detention basin which provides a level of protection for a prescribed storm pattern and loss rate. The available rainfall data is a single rain gage located off-site of the catchment.

In reviewing the rainfall data, no storms were found which precisely matched the design condition effective rainfall distribution, $e_g^D(t)$. Consequently, a storm class $\langle \xi_D \rangle$ could not be developed.

The assumption that similar storm classes, $\langle \xi_x \rangle$, have similar correlation distributions, $[\eta(s)]_x$, was then involved. By examining the available rainfall records and the runoff data from the Dominguez Wash stream gage, only 5 storms were identified which were considered similar enough to $e_g^D(t)$ to have similar correlation distributions. More data would be needed to have statistical significance; however, this information is used for demonstration purposes.

The five correlation distributions, $\eta^i(s)$, are shown in mass-curve form in Fig. 11. Each $\eta^i(s)$ is assumed to have a probability of 0.20. The $\eta^i(s)$ of Fig. 11 were derived by a least-squares fit between estimated effective rainfall from the rain gage and the stream gage using the $Q_1^i(t)$ model structure.

For the prescribed design effective rainfall storm condition (rainfall less losses) given by a $e_g^D(t)$ at the rain gage, the hydrologic model estimate for runoff is given by the distribution $[Q_1^D(t)]$ of Eq. (19).

By routing each $Q_1^D(t)$ model, (using a different $\eta^i(s)$ for each trial), through the detention basin, a different demand on the basin volume is determined. Figures 12 and 13 show the resulting distribution of $Q_1^D(t)$ and the associated detention basin volume requirements, respectively. Also shown in Fig. 13 are confidence estimates from the modeling results.

CONCLUSIONS

A lower bound for estimating the distribution of uncertainty in surface runoff modeling output is advanced. The bound is based on a linear unit hydrograph approach, which utilizes an arbitrary number of catchment subdivisions into subareas, a linear routing technique for channel flow effects, a variable effective rainfall distribution over the catchment, and calibration parameter distributions developed

in correlating rainfall-runoff data by the model. Because all hydrologic parameters (e.g., subarea unit hydrographs, channel routing parameters, effective rainfall distribution factors) vary on a storm basis, the unit hydrograph methodology is a reasonable approximation for assessing uncertainty in hydrologic modeling estimates. The uncertainty bound developed reflects the dominating influence of the unknown rainfall distribution over the catchment and is expressed as a distribution function which can be reduced only by supplying additional rainfall-runoff data. It is recommended that this uncertainty distribution be included in flood control design studies in order to incorporate prescribed levels of confidence in flood protection facilities.

Also developed in this paper is the conclusion that the single area UH modeling structure represents a highly complex link-node model where all parameters are validated by data. The single area model UH integrates several effects occurring during storm event i; namely, (1) variation in the individual subarea UH across storm events, (2) the distribution of the individual runoff hydrograph channel routing effects, and (3) the variations in the effective rainfall magnitude, timing, and pattern shape over the catchment. When correlating stream gage runoff to effective rainfall, the single area UH determined by calibration will include the above described effects.

In contrast, using a highly discretized model during calibration will result in a 'rigid' UH which transfer the unknown variations in the above cited effects to the model's effective rainfall distribution, resulting in a less reliable calibration of the loss functions parameters.

The correlation of the effective rainfall to the runoff hydrograph from the catchment R will result in a different UH (for the single area model) for each storm event. However, the resulting collection of UH's reflect the dominating uncertainty in the variation in the magnitude, timing, and shape of the effective rainfall distribution over R. When the data base consists of only a single rain gage and stream gage these three uncertainties cannot be reduced by including additional complexities into the hydrologic model (e.g., subareas linked by hydraulic routing submodels, additional soil-moisture accounting algorithms, etc.). Only additional measured rainfall-runoff data within the catchment R will reduce the uncertainty. Without this additional data, the uncertainty in the effective rainfall over R will remain and should be included in flood control design and planning studies by the development of confidence levels in the modeling results.

APPENDIX I - REFERENCES

1. Beard, L. and Chang, S, Urbanization Impact on Stream Flow, ASCE, Journal of the the Hydraulics Division, June, 1979.

2. Doyle, Jr., W. H., Shearman, J. O., Stiltner, G. J., and Krug, W. R., A Digital Model for Streamflow Routing by Convolution Methods, U.S. Geological Survey, Water-Resources Investigation Report 83-4160, 1983.

3. Garen, D. and Burges, S., Approximate Error Bounds for Simulated Hydrographs, ASCE Journal of the Hydraulics Division, Vol. 107, No. 11, Nov., 1981.

4. Loague, K. and Freeze, R., A Comparison of Rainfall-Runoff Modeling Techniques on Small Upland Catchments, Water Resources Research, Vol. 21, No. 2, Feb., 1985.

5. Nash, J. and Sutcliffe, J., River Flow Forecasting Through Conceptual Models, Part I - A Discussion of Principles, Journal of Hydrology, Vol. 10, 1970.

6. Schilling, W. and Fuchs, L., Errors in Stormwater Modeling - A Quantitative Assessment, ASCE Journal of Hydraulic Engineering, Vol. 112, No. 2, Feb., 1986.

7. Troutman, B., An Analysis of Input in Precipitation - Runoff Models Using Regression with Errors in the Independent Variables, Water Resources Research, Vol. 18, No. 4, Aug., 1982.

APPENDIX II - NOTATION

The following notation is used in this paper:

α_{k_1} = timing offsets for channel link #1 used in the linear routing technique

$\alpha^o_{k_1}$ = α_{k_1} corresponding to storm class $<\xi_o>$

λ^i_{jk} = effective rainfall proportion factors for subarea R_j for storm i

θ^i_{jk} = effective rainfall timing offsets for subarea R_j for storm i

$\phi_j{}^i(s)$ = subarea unit hydrograph (UH) for subarea R_j and storm i

$<\xi_o>$ = specific storm class

$<\xi_x>$ = arbitrary storm class

$\eta^i(s)$ = correlation distribution between measured effective rainfall and measured runoff, for storm i, using a Voltera integral model structure

$\tau_j{}^i$ = translation timing offset for channel link j and storm i

ω_1, ω_2 = area weighting factors

a_{k_1} = proportion factors for linear routing technique, used for channel link #1

A_1 = subarea R_1 area

D = design condition

$e_g{}^i(t)$ = effective rainfall measured at the rain gage site, for storm i

$e_g{}^o(t)$ = the effective rainfall corresponding to storm class $<\xi_o>$, measured at the rain gage

$e_j{}^i(t)$ = subarea R_j effective rainfall for storm i

i = storm event i

j,k = indices

I(t) = inflow hydrograph for linear routing

$O(t)$ = outflow hydrograph for linear routing

$P_g^i(t)$ = rainfall measured at the rain gage site, for storm i

$Q_g^i(t)$ = runoff hydrograph, for storm i, measured at the stream gage

$Q_g^{oi}(t)$ = a $Q_g^i(t)$ resulting from an element of storm class $<\xi_o>$

$q_j^i(t)$ = runoff hydrograph from subarea R_j, for storm i

$Q_m^i(t)$ = m-subarea link-node model output for storm i

R = total catchment

R_j = subarea in R

s,t = temporal & integration variables

UH = unit hydrograph

$[Z]$ = distribution for random variable Z

$[Z]_o$ = $[Z]$ for storm class $<\xi_o>$

$\hat{Z}$ = estimate for Z

$\tilde{Z}$ = calibrated estimate for Z

$\bar{Z}$ = mean value for Z

$<k>$ = vector notation for subscript sequence, k

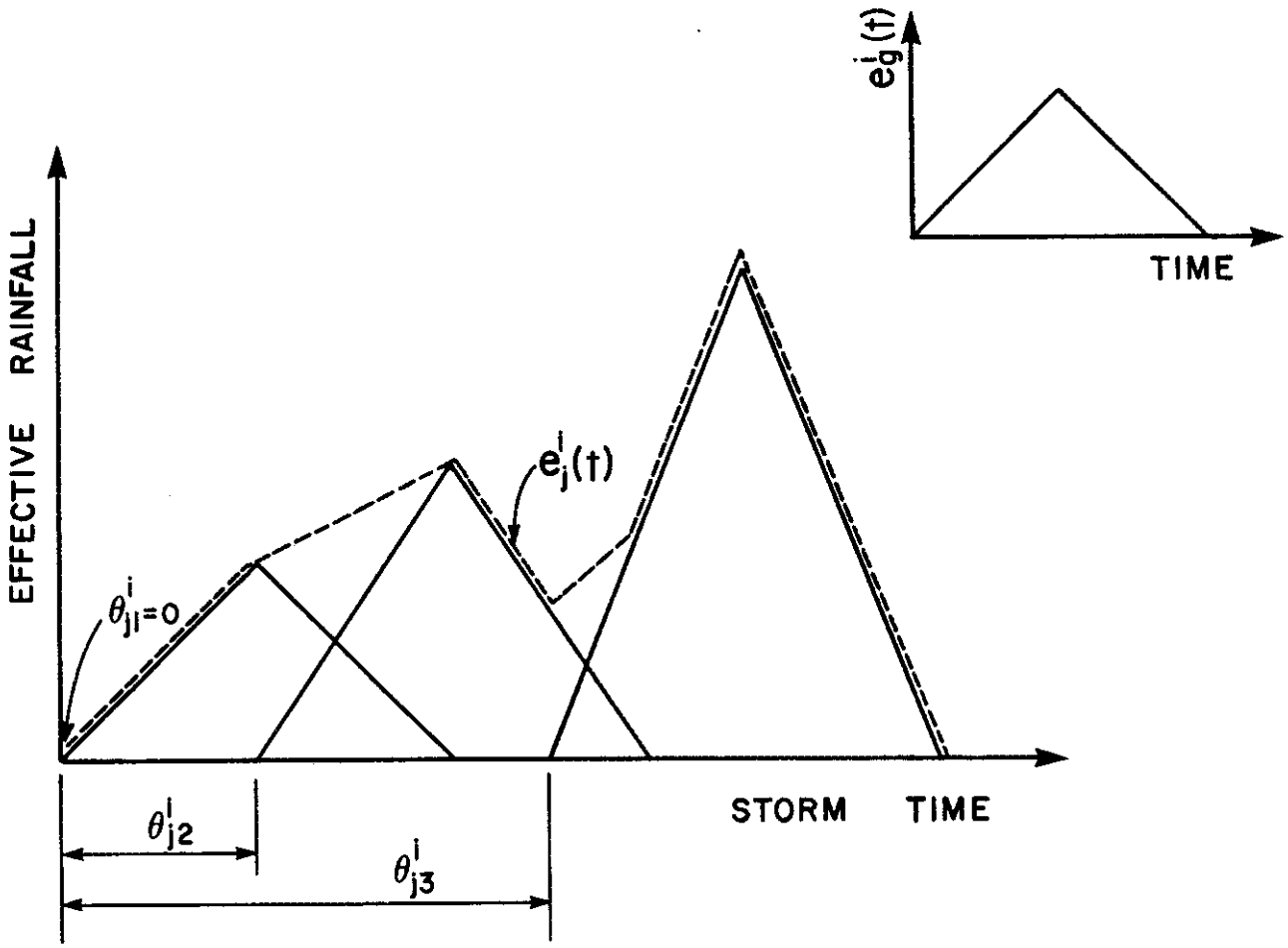

Fig. 1. Subarea Effective Rainfall as a Linear Combination of Rain Gage Measured Effective Rainfall

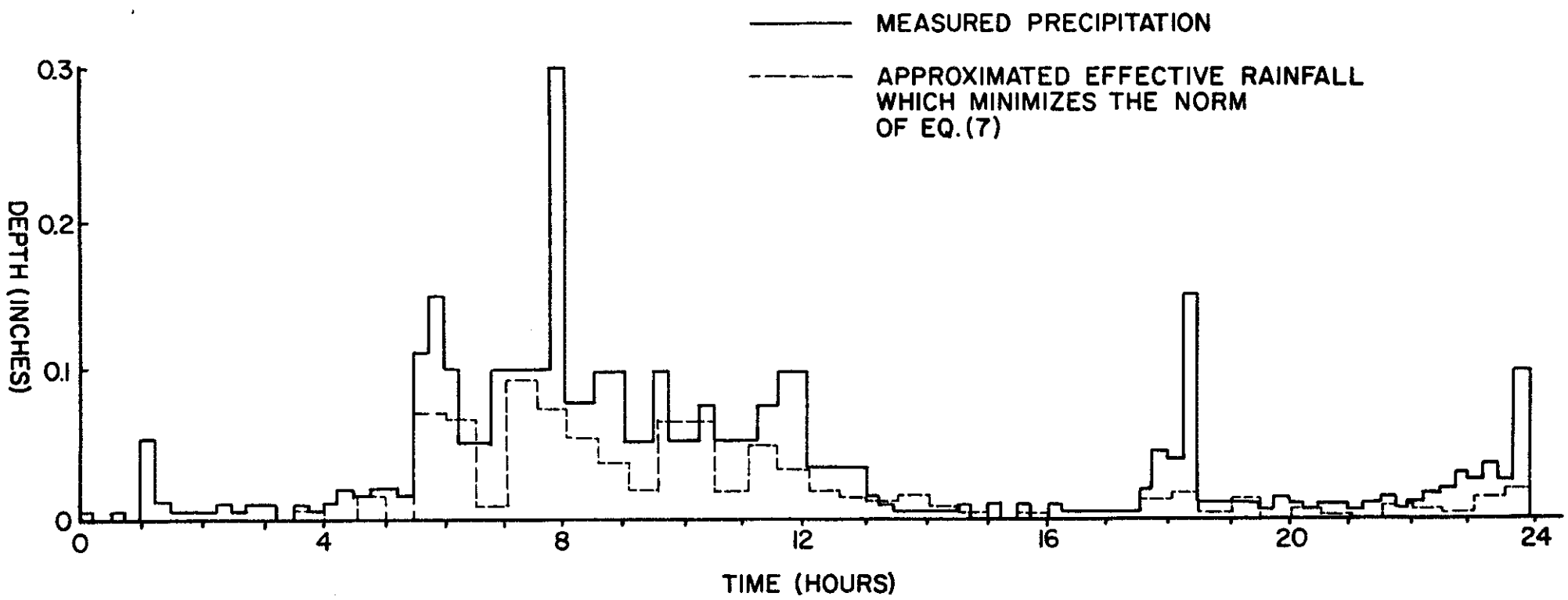

Fig. 2a. Subarea R_1 Effective Rainfalls, $e_1^i(t)$, for March 1 Storm, which Minimize the Approximation Error of Eq. (7). Note that $e_1^i(t)$ is not derived from the precipitation, but is derived by correlating measured runoff to the assumed unit hydrograph for subarea R_1.

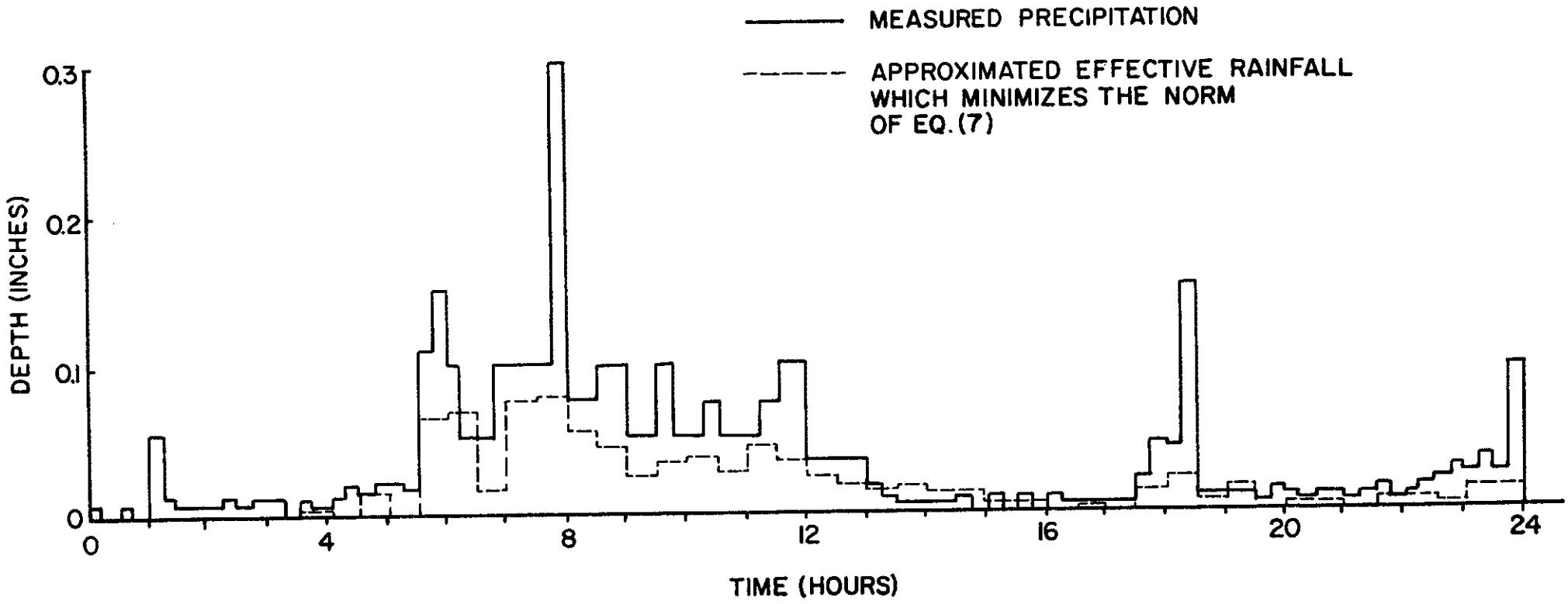

Fig. 2b. Subarea R_2 Effective Rainfalls, $e_2^i(t)$.
Note that $e_2^i(t)$ differs from $e_1^i(t)$ of Fig. 2a.

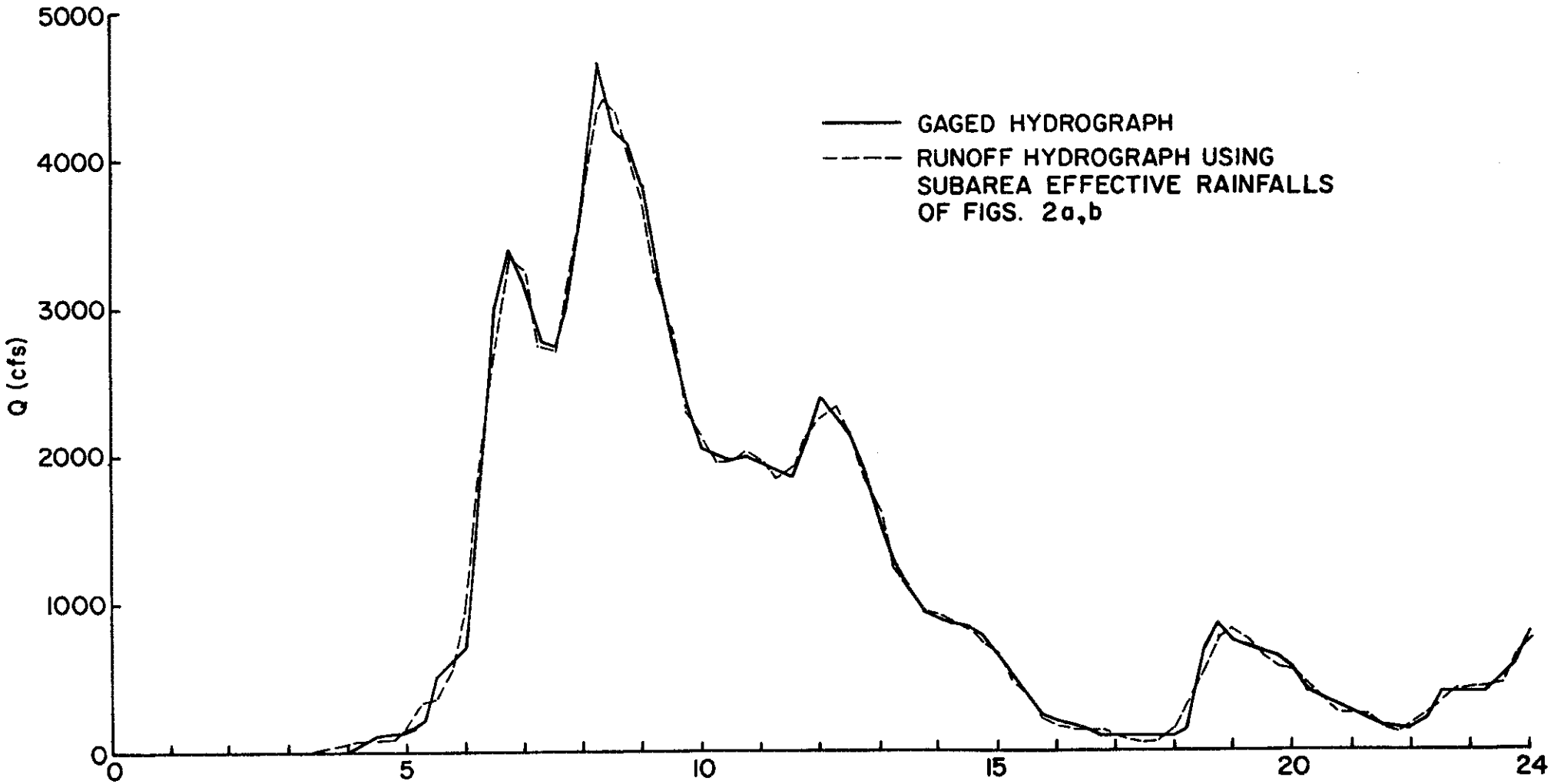

Fig. 3. Comparison of Measured Runoff Hydrograph, $Q_g^i(t)$, and Modeled Runoff, $Q_2^i(t)$, using Subarea Effective Rainfalls shown in Figs. 2a,b and Derived From Eq. (7).

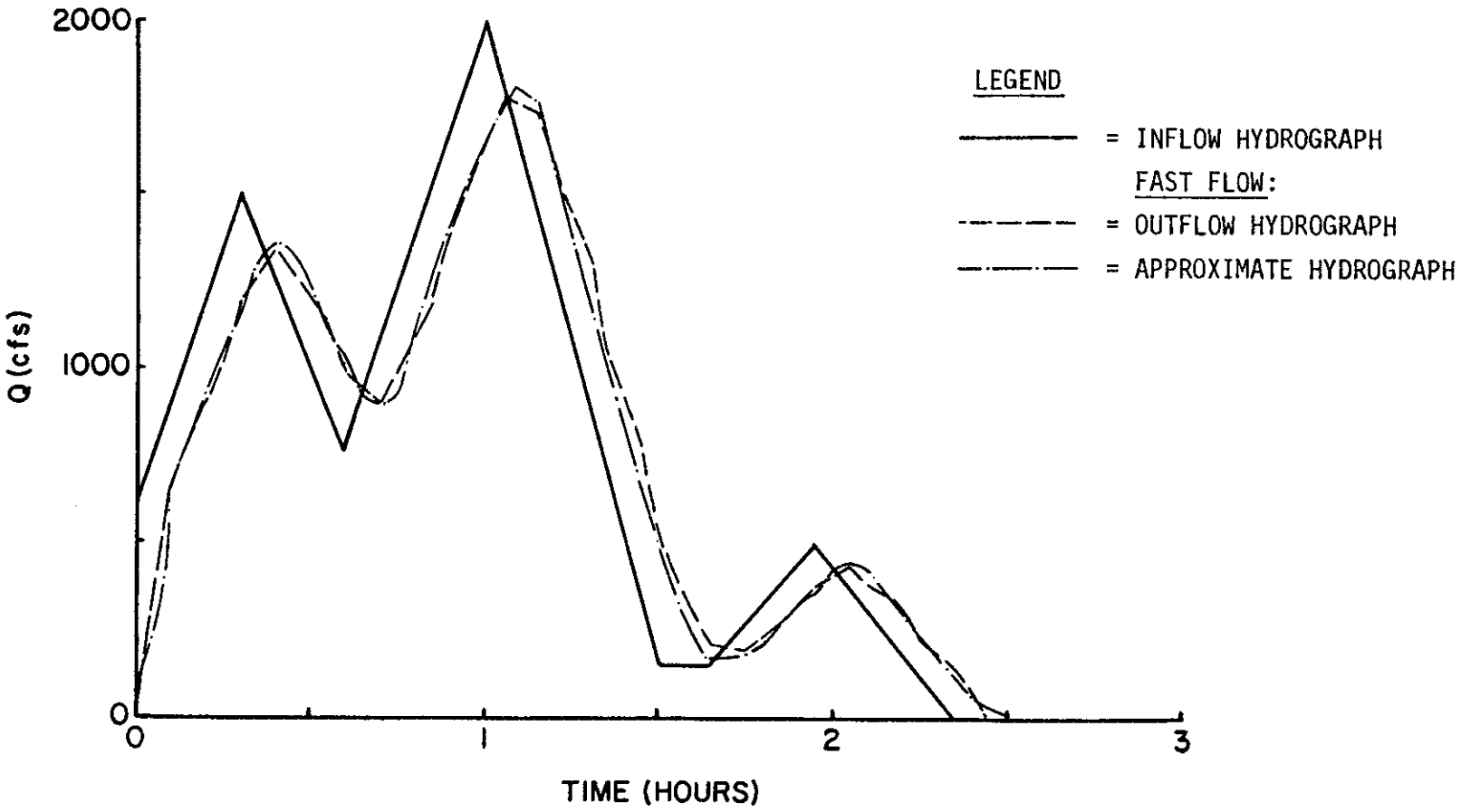

Fig. 4a. Fast Flow Linear Routing Approximation Calibration Using Four Translates.

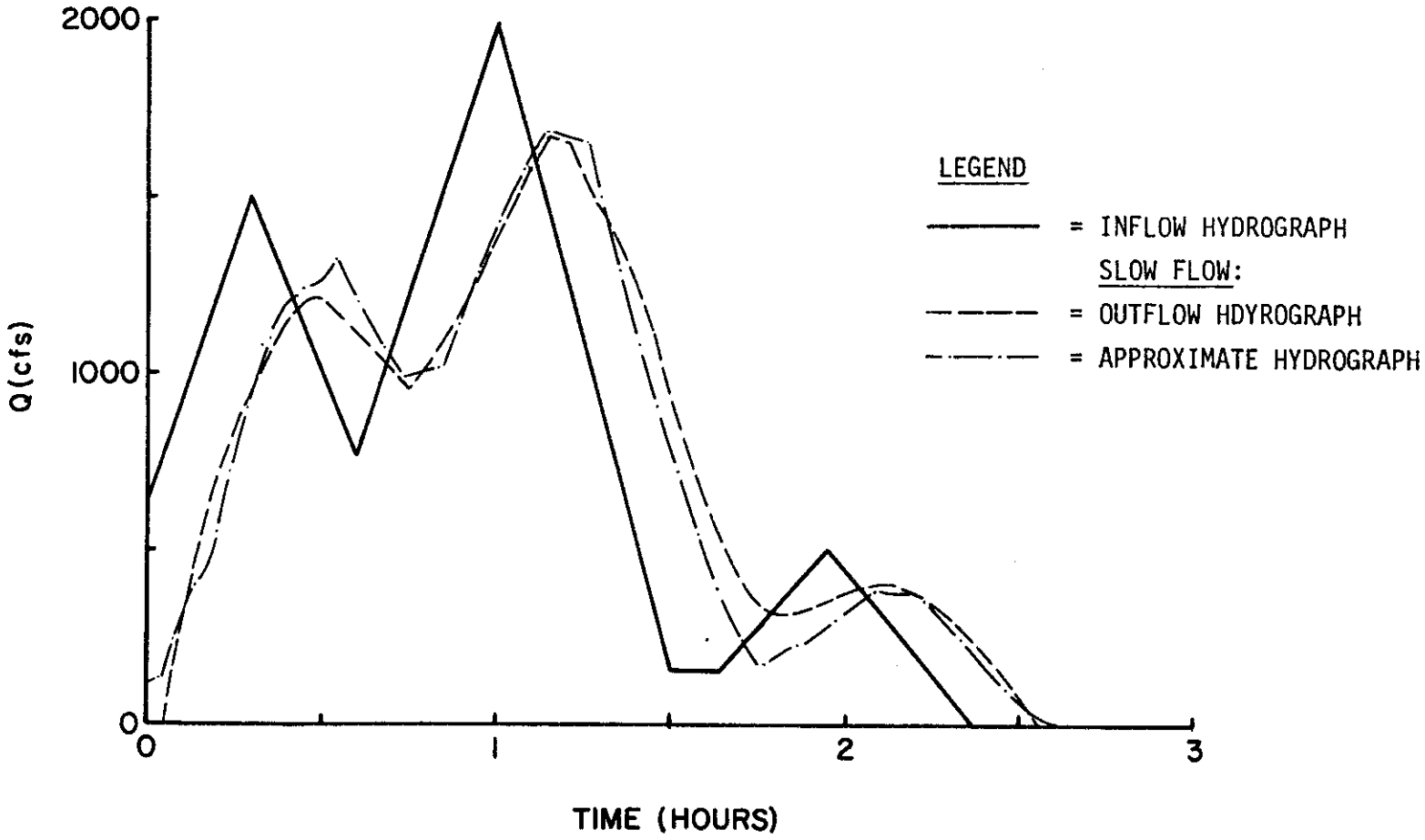

Fig. 4b. Slow Flow Linear Routing Approximation Calibration Using Four Translates.

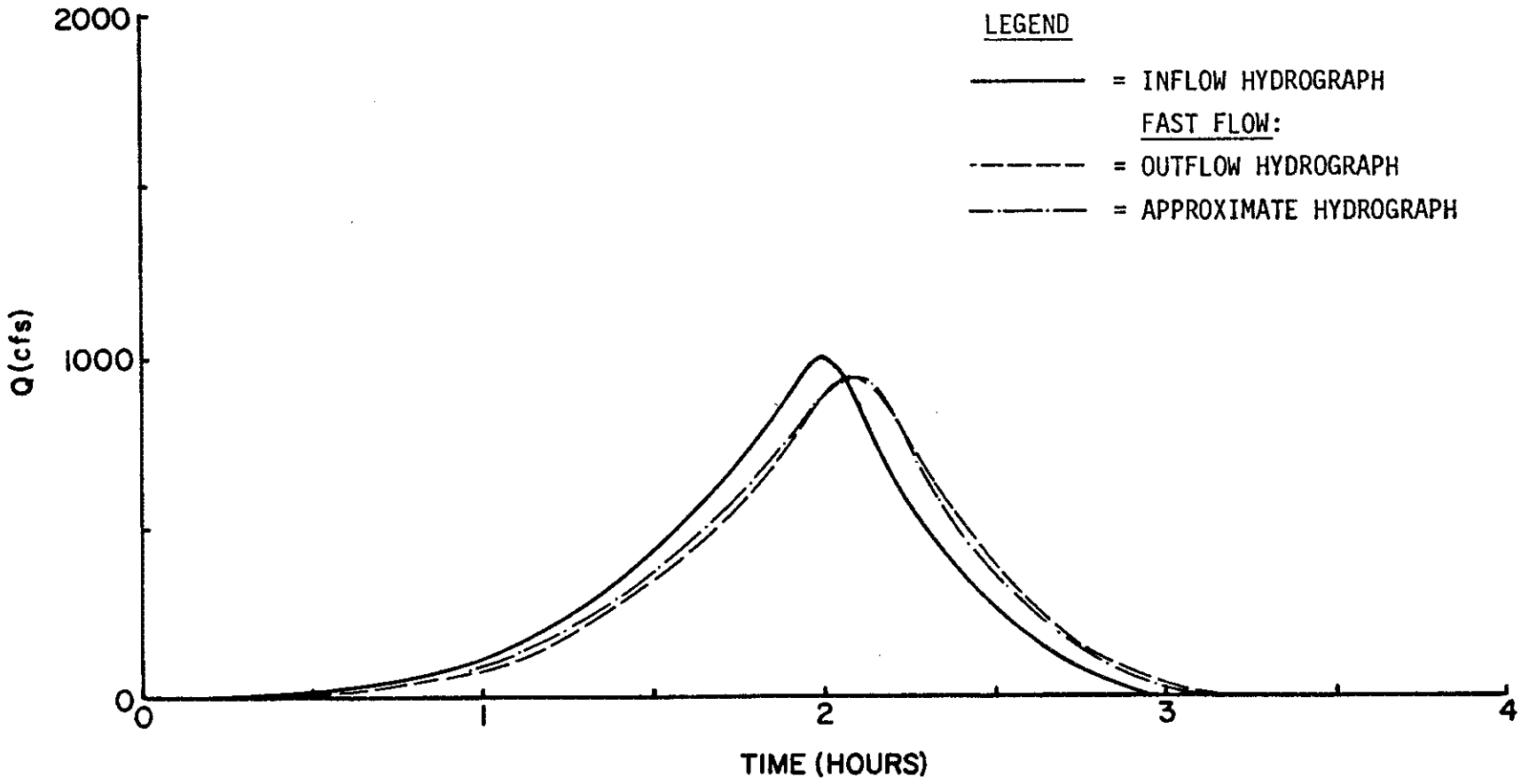

Fig. 5a. Fast Flow Linear Routing Model Verification Test (1 of 4).
(Model was calibrated in Fig. 4a.)

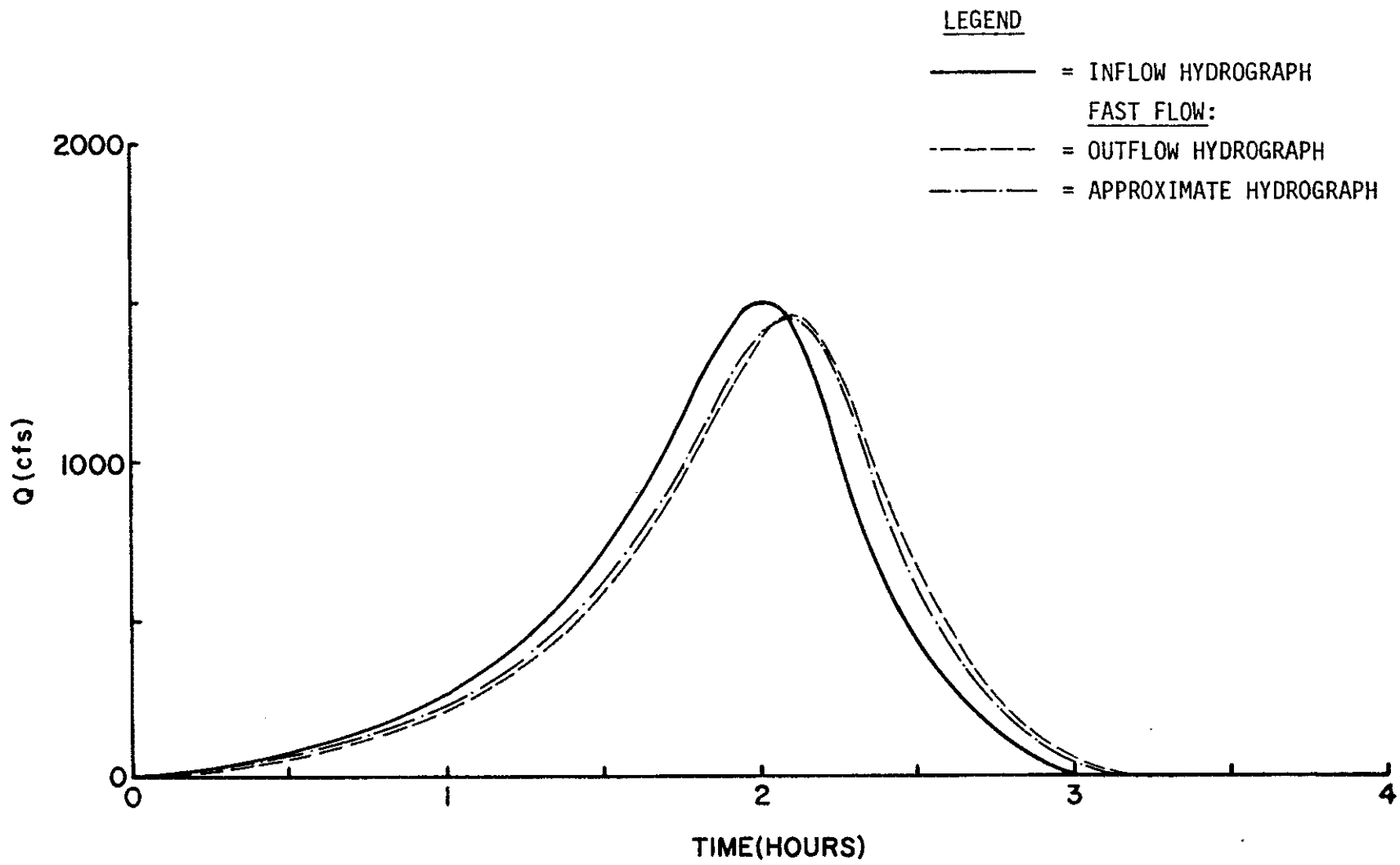
LEGEND
= INFLOW HYDROGRAPH
FAST FLOW:
= OUTFLOW HYDROGRAPH
= APPROXIMATE HYDROGRAPH
2000
1000
0
Q(cfs)
0
1
2
3
4
TIME(HOURS)

Fig. 5a. (2 of 4)

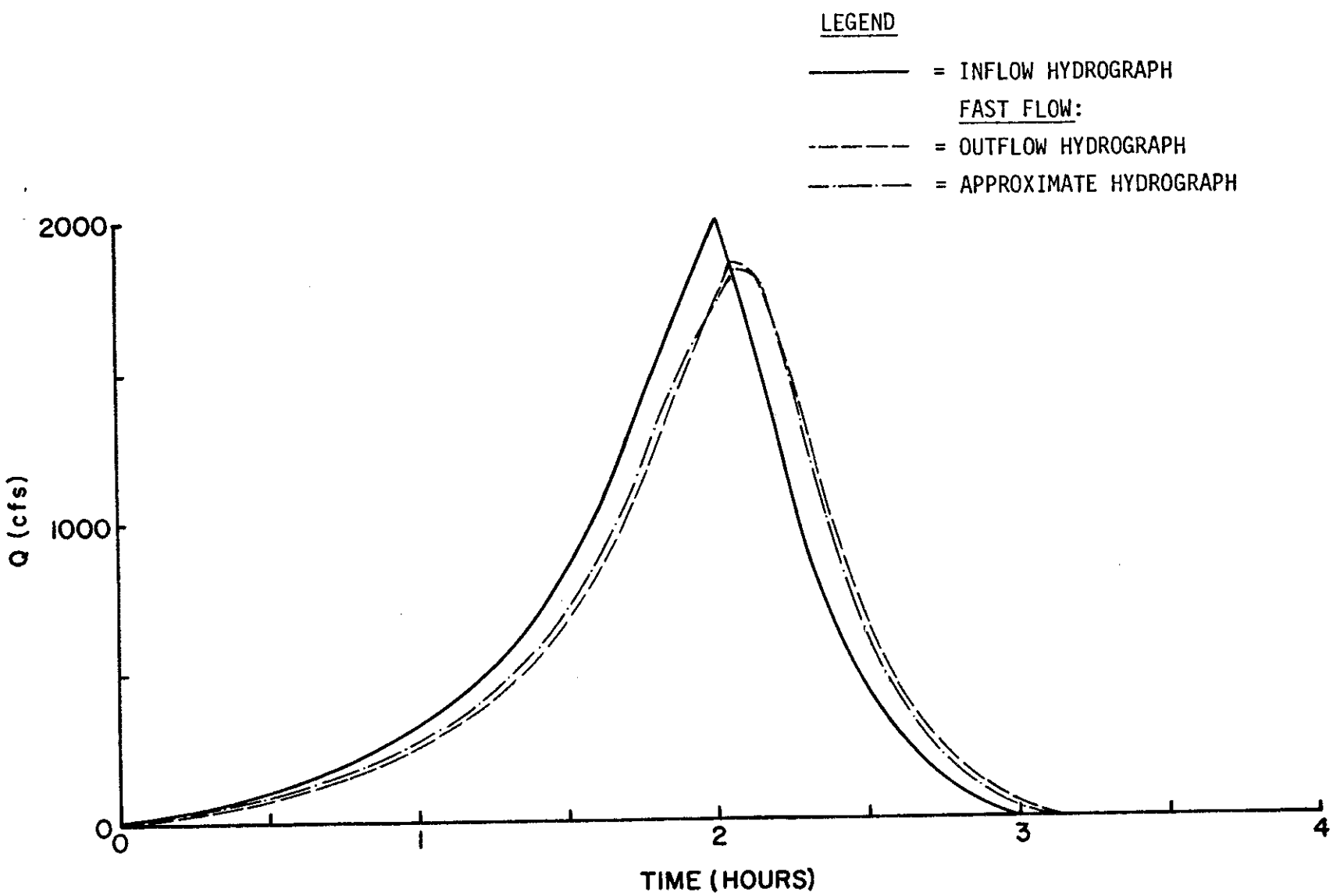
LEGEND
= INFLOW HYDROGRAPH
FAST FLOW:
= OUTFLOW HYDROGRAPH
= APPROXIMATE HYDROGRAPH
2000
1000
0
Q (cfs)
0
1
2
3
4
TIME (HOURS)

Fig. 5a. (3 of 4)

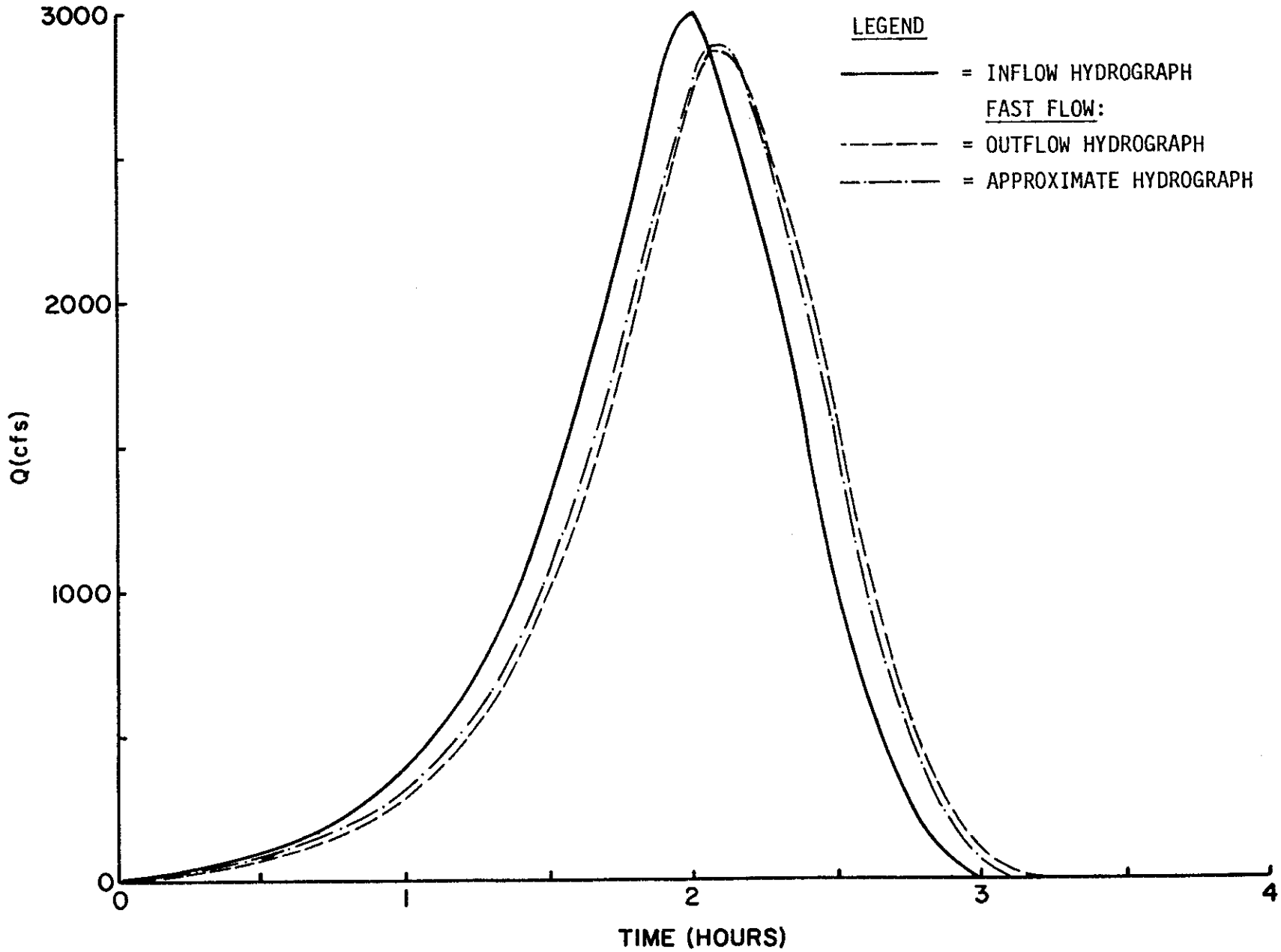
3000
2000
1000
0
Q(cfs)
0
1
2
3
4
TIME (HOURS)
LEGEND
= INFLOW HYDROGRAPH
FAST FLOW:
= OUTFLOW HYDROGRAPH
= APPROXIMATE HYDROGRAPH

Fig. 5a. (4 of 4)

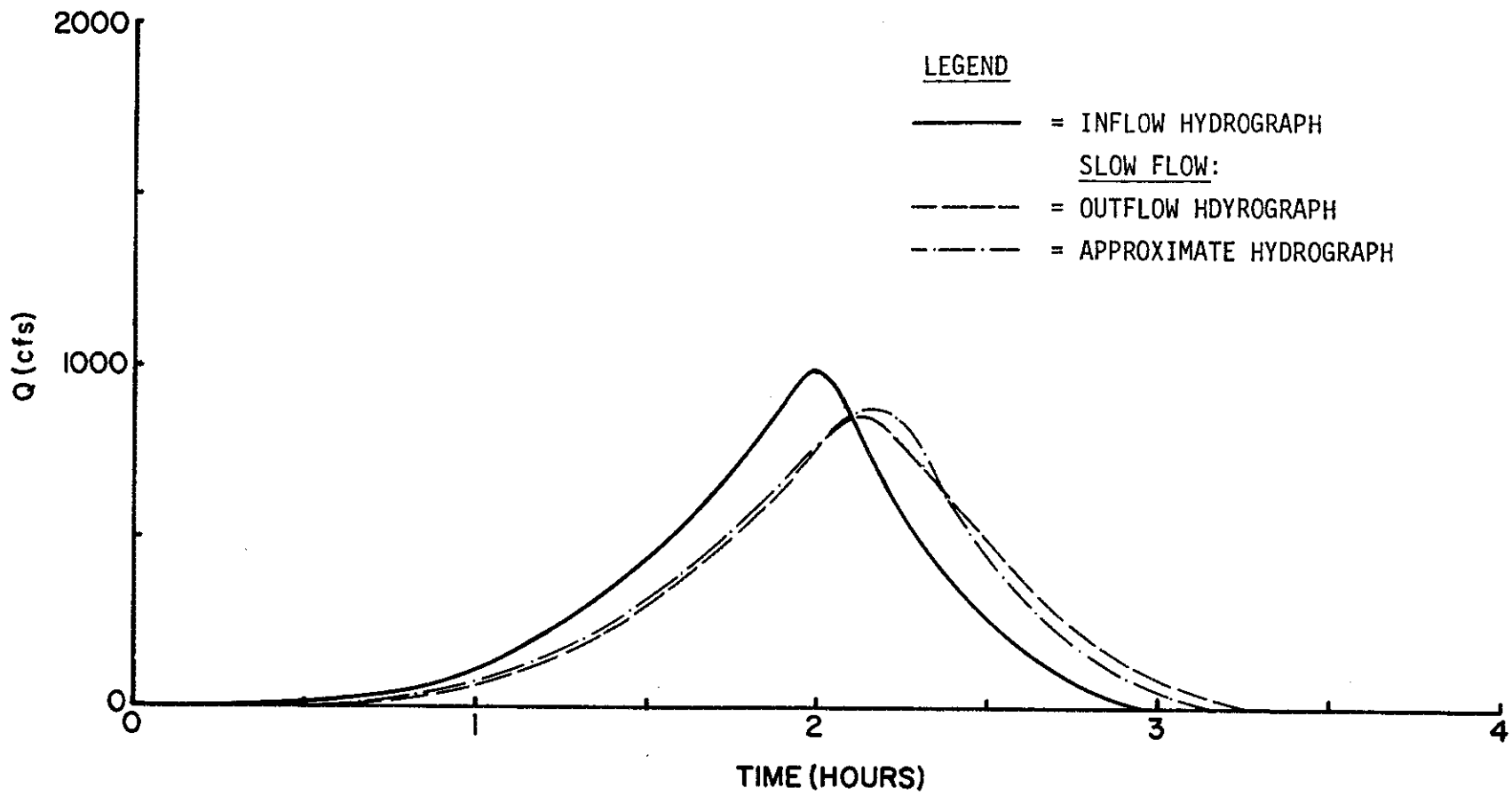

Fig. 5b. Slow Flow Linear Routing Model Verification Test (1 of 4).
(Model was calibrated in Fig. 4b.)

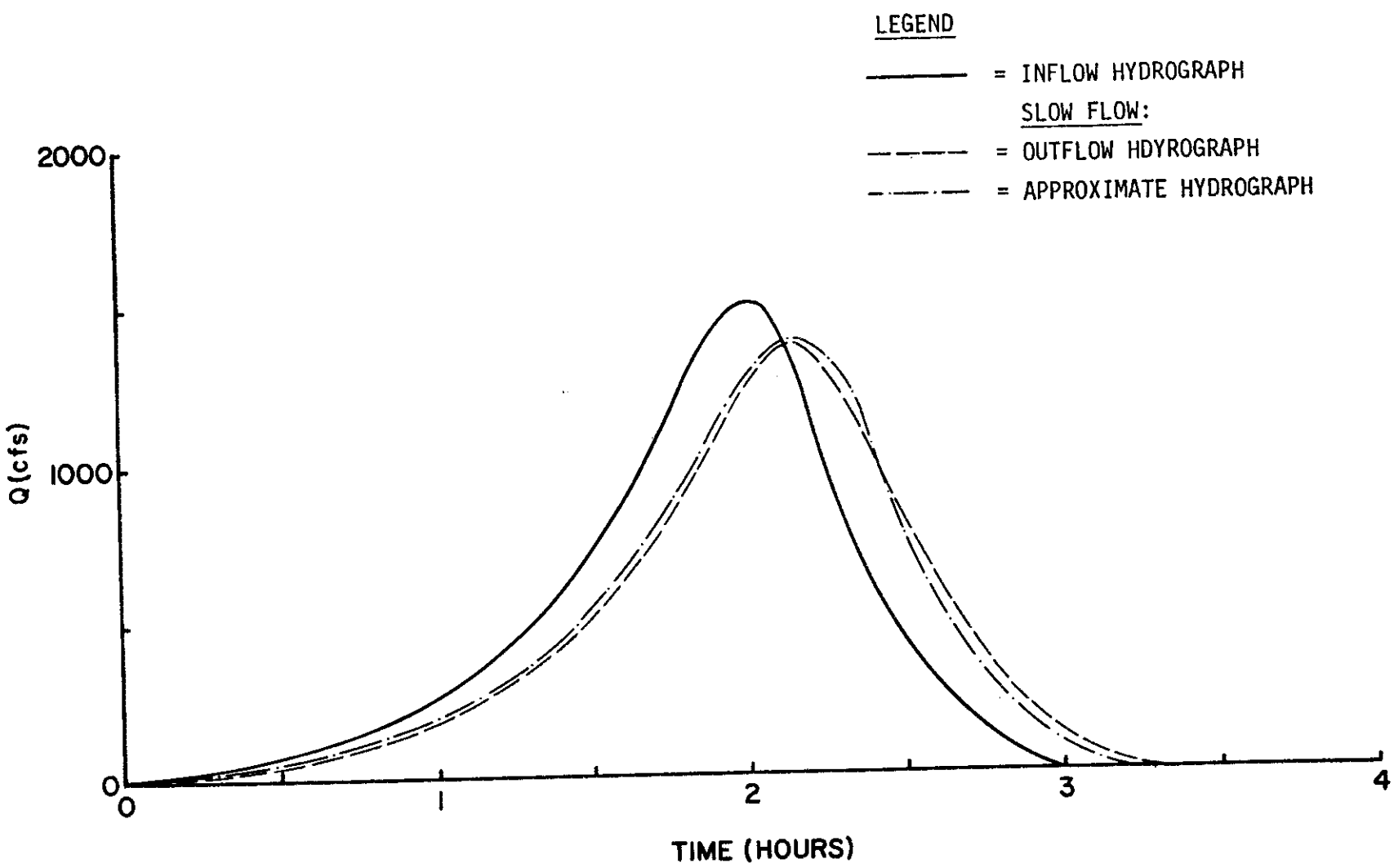
LEGEND
= INFLOW HYDROGRAPH
SLOW FLOW:
= OUTFLOW HDYROGRAPH
= APPROXIMATE HYDROGRAPH
2000
1000
0
Q(cfs)
0
1
2
3
4
TIME (HOURS)

Fig. 5b. (2 of 4)

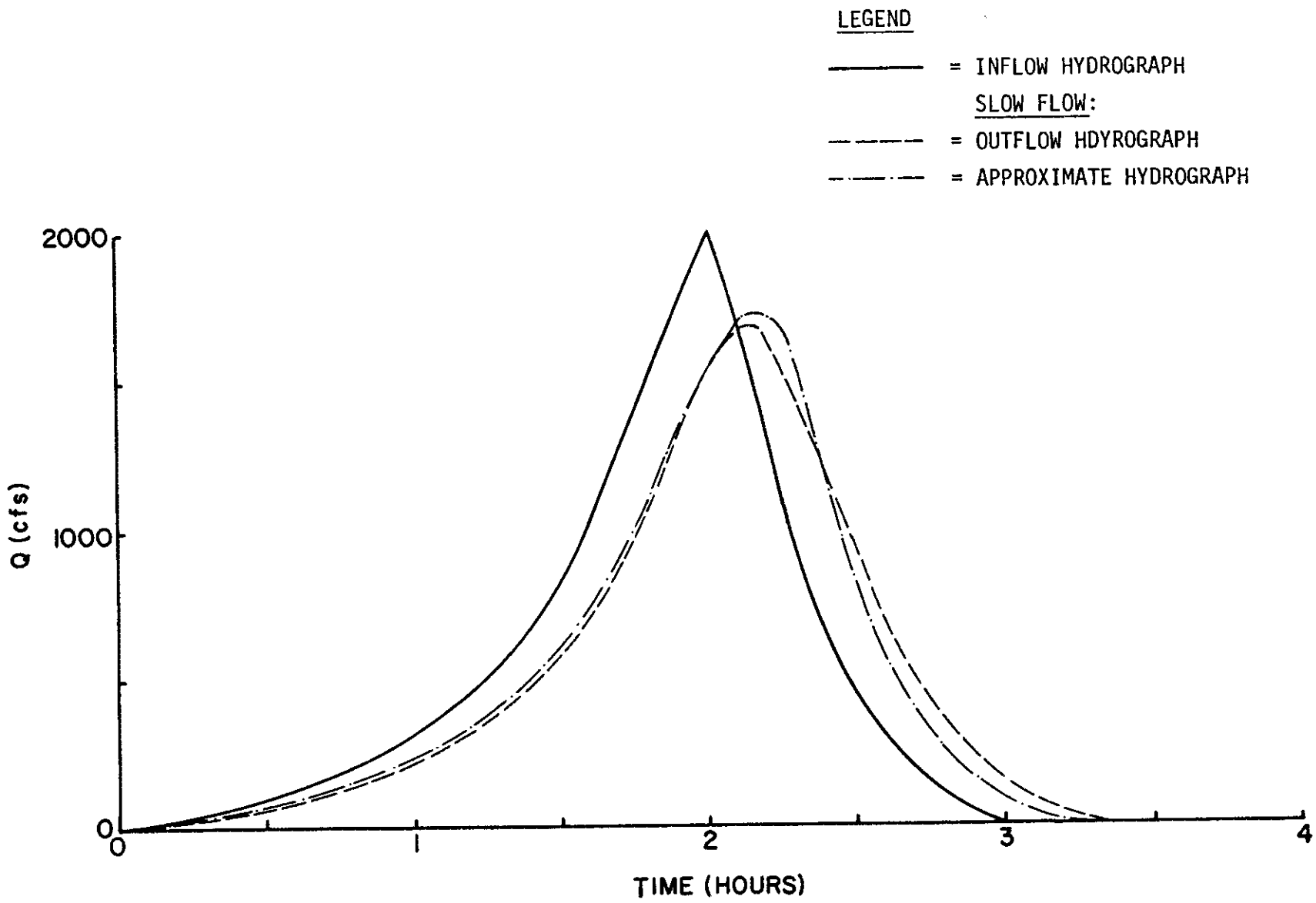
LEGEND
= INFLOW HYDROGRAPH
SLOW FLOW:
= OUTFLOW HDYROGRAPH
= APPROXIMATE HYDROGRAPH
2000
1000
0
Q (cfs)
0
1
2
3
4
TIME (HOURS)

Fig. 5b. (3 of 4)

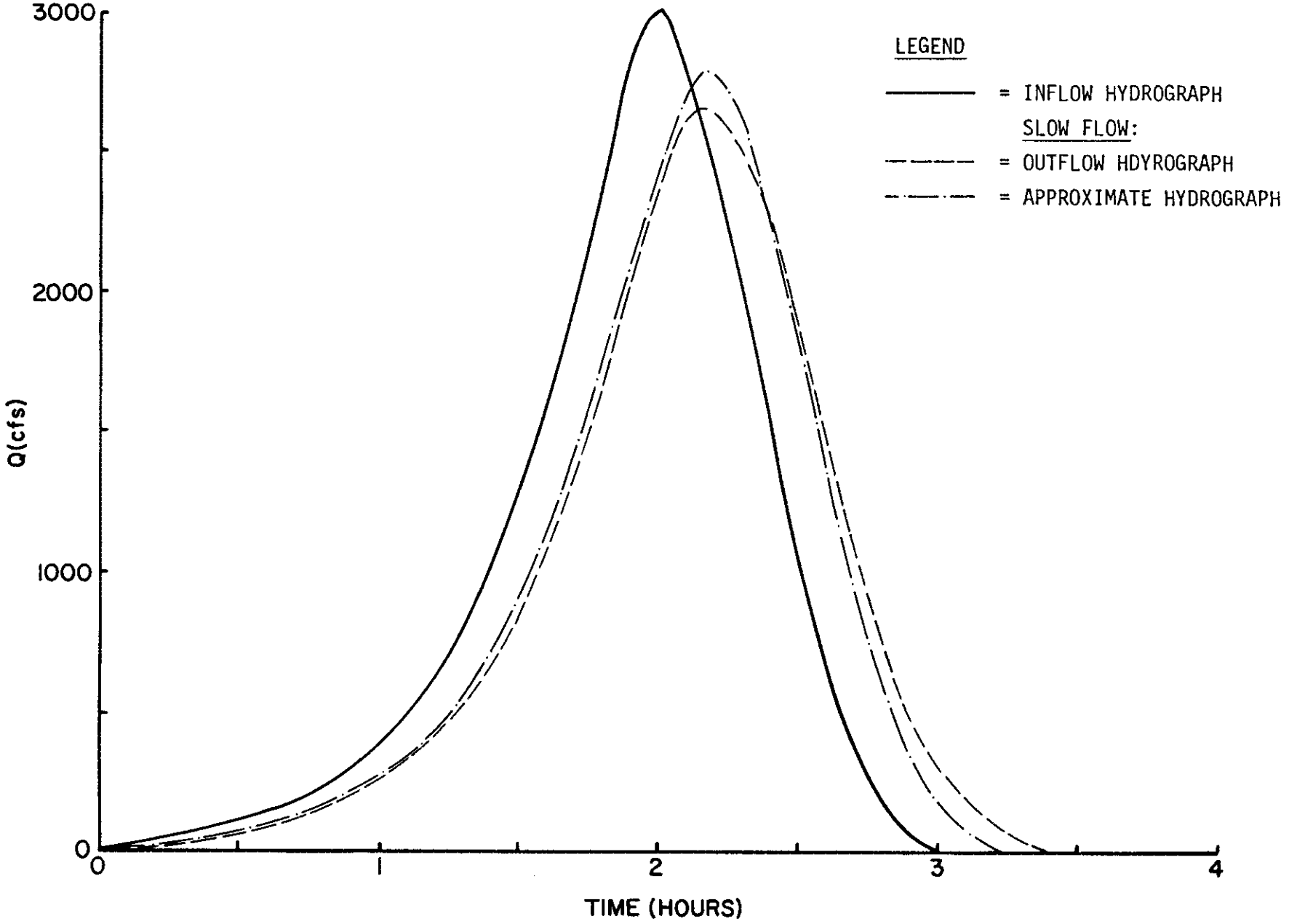
3000
2000
1000
0
Q(cfs)
0
1
2
3
4
TIME (HOURS)
LEGEND
= INFLOW HYDROGRAPH
SLOW FLOW:
= OUTFLOW HDYROGRAPH
= APPROXIMATE HYDROGRAPH

Fig. 5b. (4 of 4)

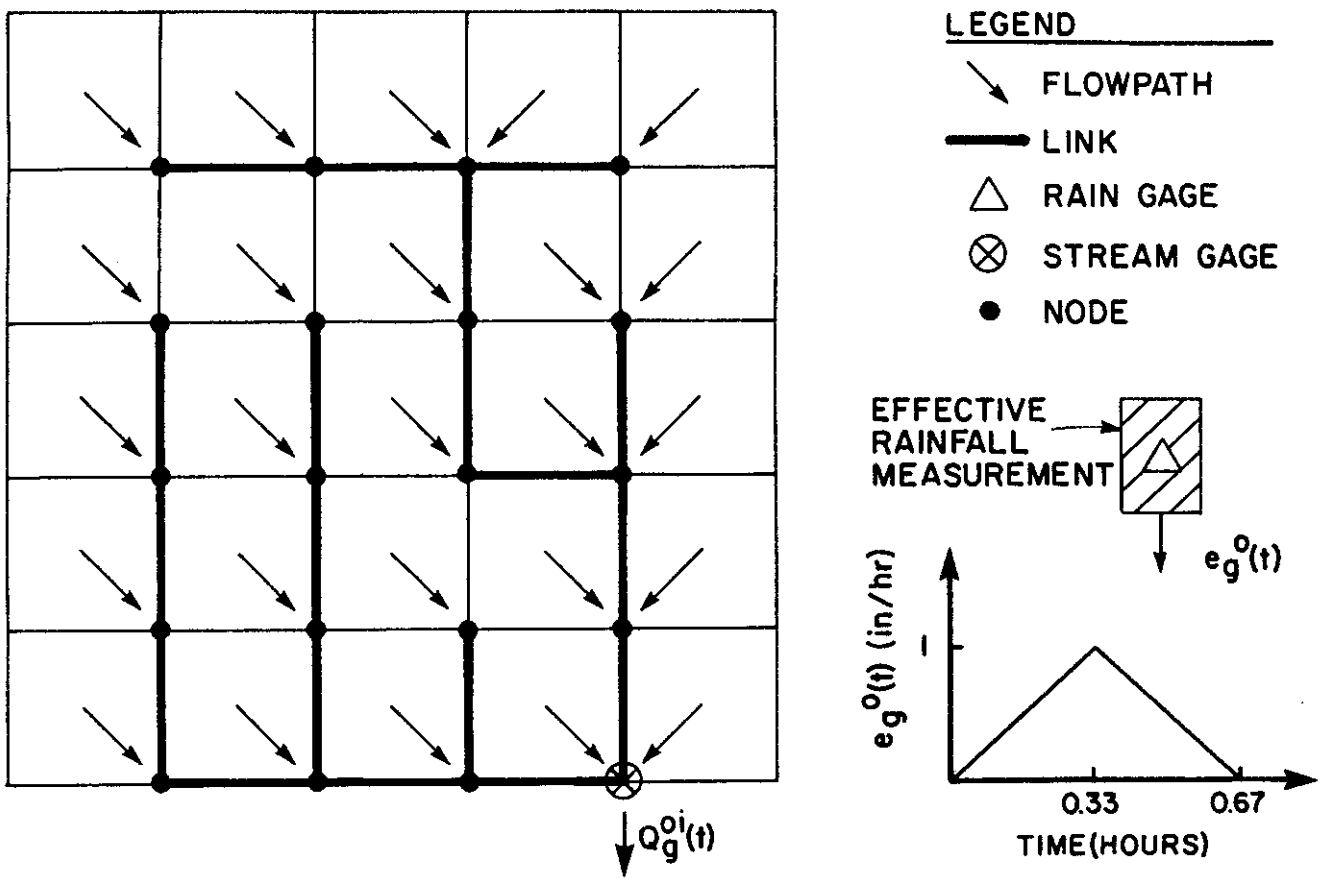

Fig. 6. Application Problem Schematic

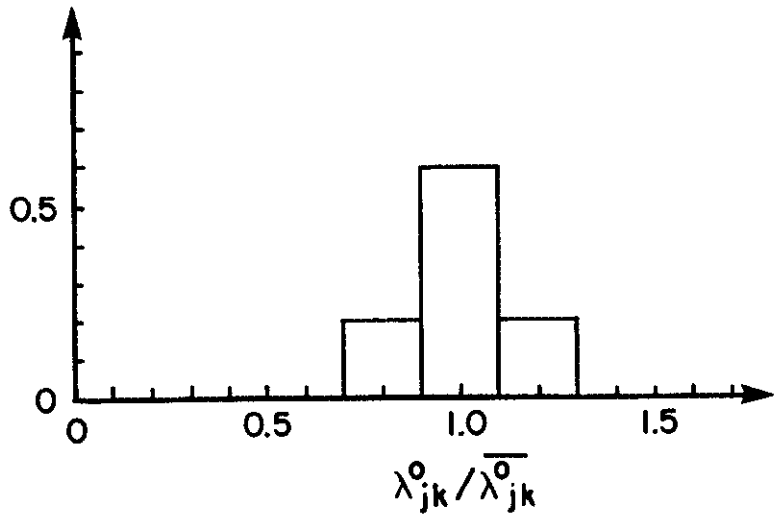

Fig. 7a. Frequency Distribution for $\lambda^{oi}{}_{jk} / \overline{\lambda^{oi}{}_{jk}}$
(see table 1 for subarea $\overline{\lambda^{oi}{}_{jk}}$)

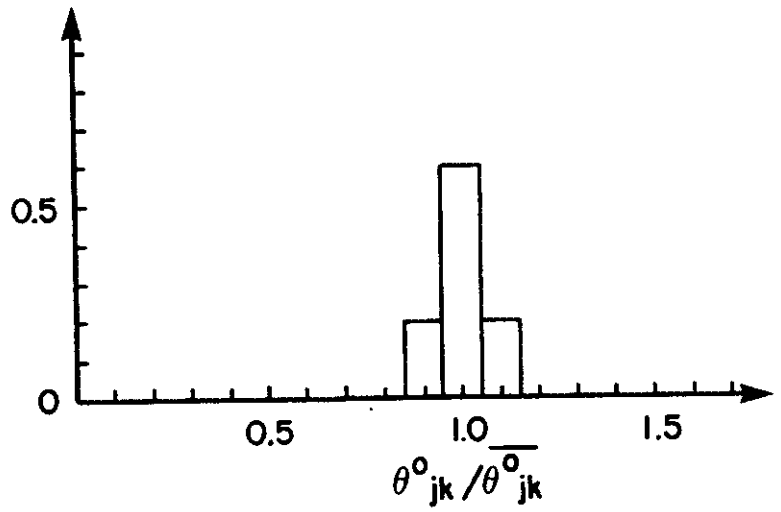

Fig. 7b. Frequency Distribution for $\theta^{oi}{}_{jk}$
(see table 1 for subarea $\overline{\theta^{oi}{}_{jk}}$)

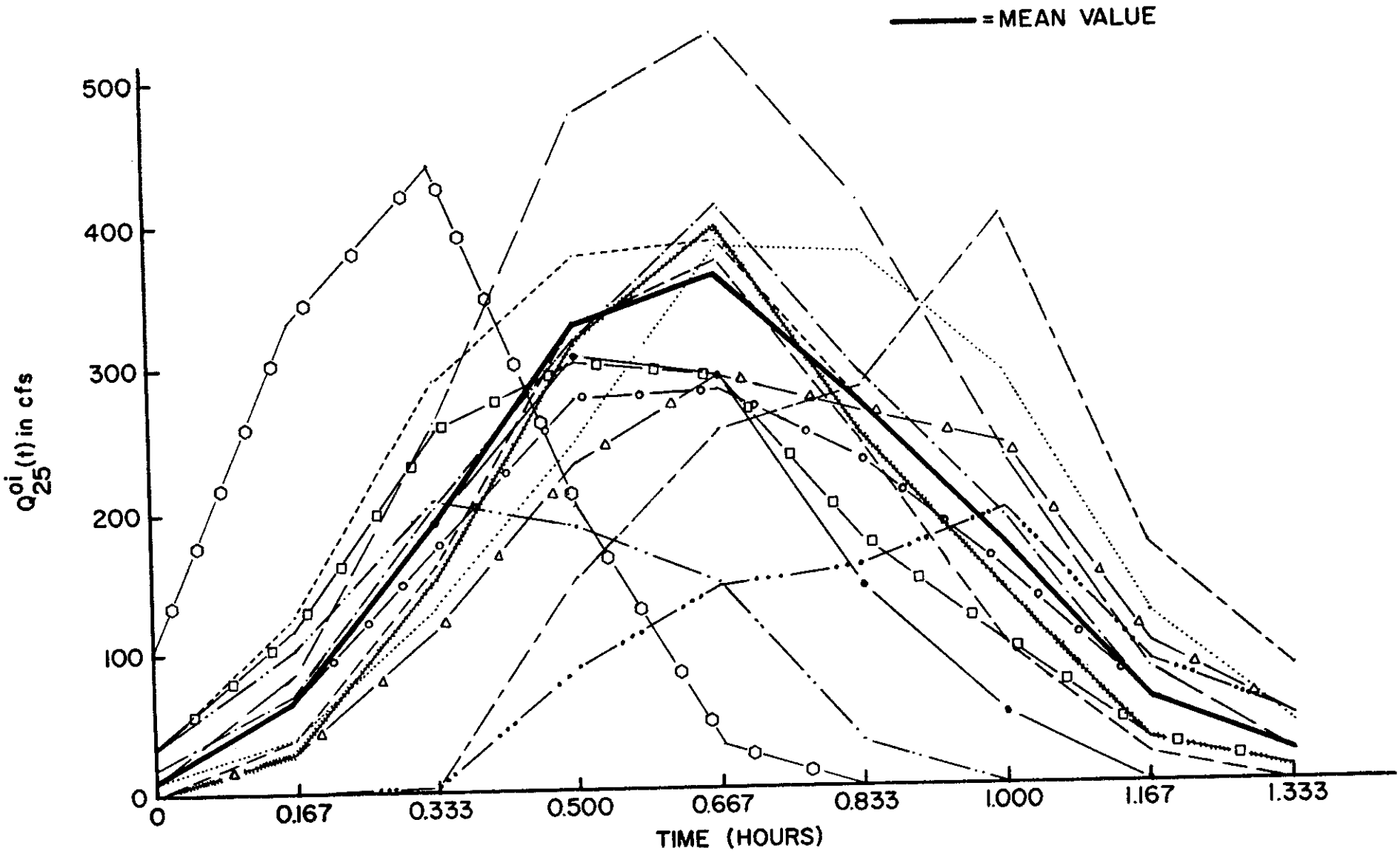

Fig. 8. Runoff Hydrographs, $Q_{25}^{oi}(t)$ using 25-subarea (Fig. 6) link-node model of Eq. (15) with effective rainfalls in subareas according to Eq. (1) and Table 1.

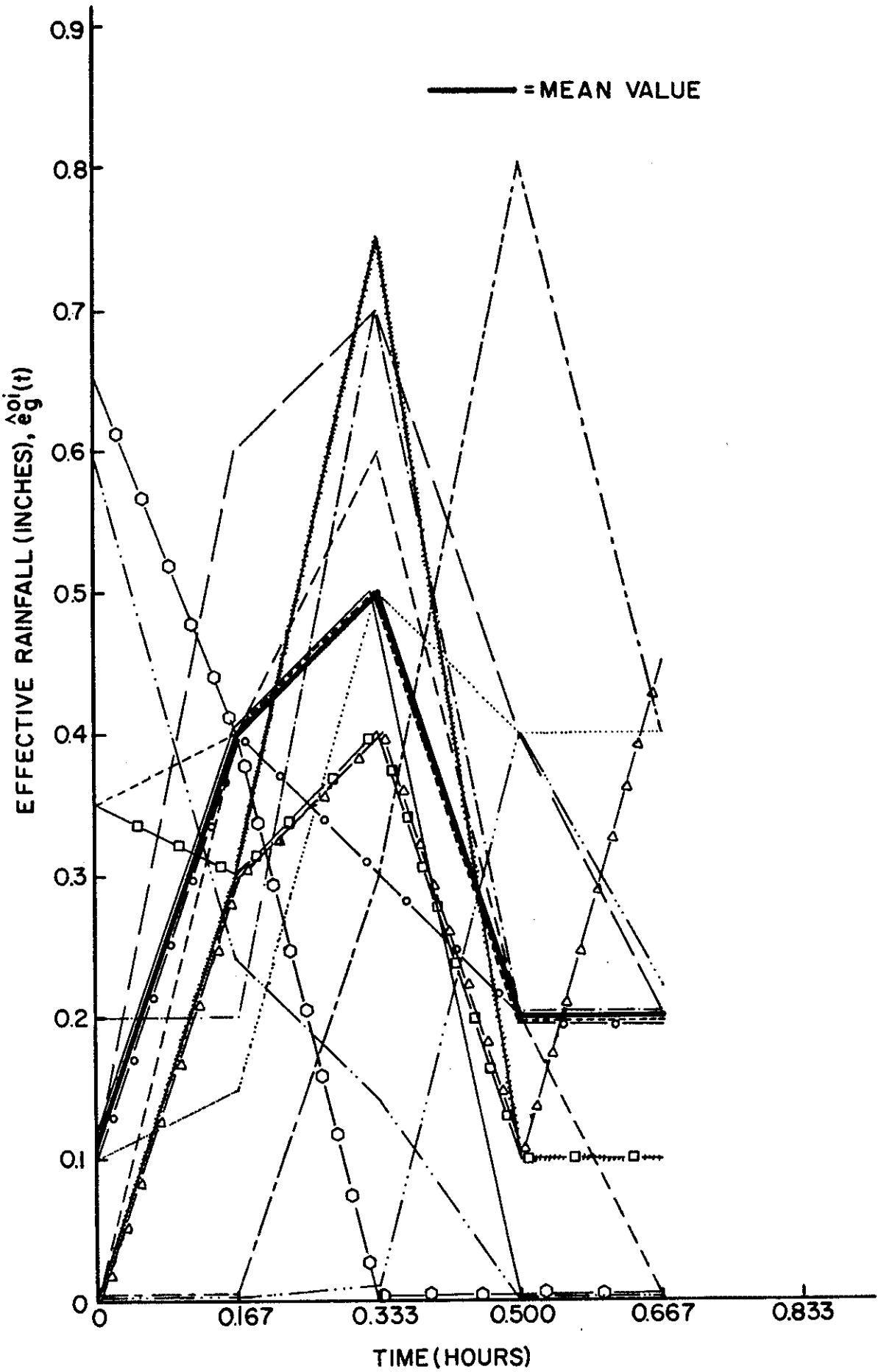

Fig. 9. Effective Rainfalls, $\hat{e}_g^{oi}(t)$, needed to develop Fig. 8 Runoff Hydrographs, $Q_{25}^{oi}(t)$, given the fixed Unit Hydrograph, $\hat{n}_o(s)$, corresponding to the 25-subarea model of Fig. 6 and Uniform Rainfalls across the Catchment ($[\lambda_{jk}] \equiv \hat{\lambda}_j$, $[\theta_{jk}] \equiv 0$).

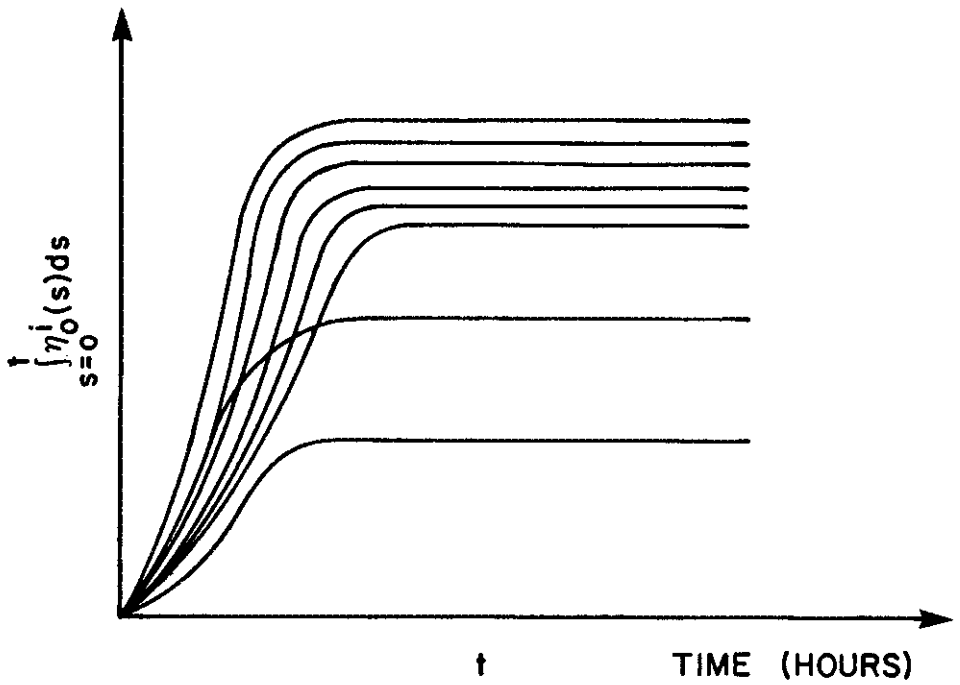

Fig. 10. Example Summation Graphs of Distributions, $\hat{\eta}_o^i(s)$ for Storms in Class $<\xi_o>$

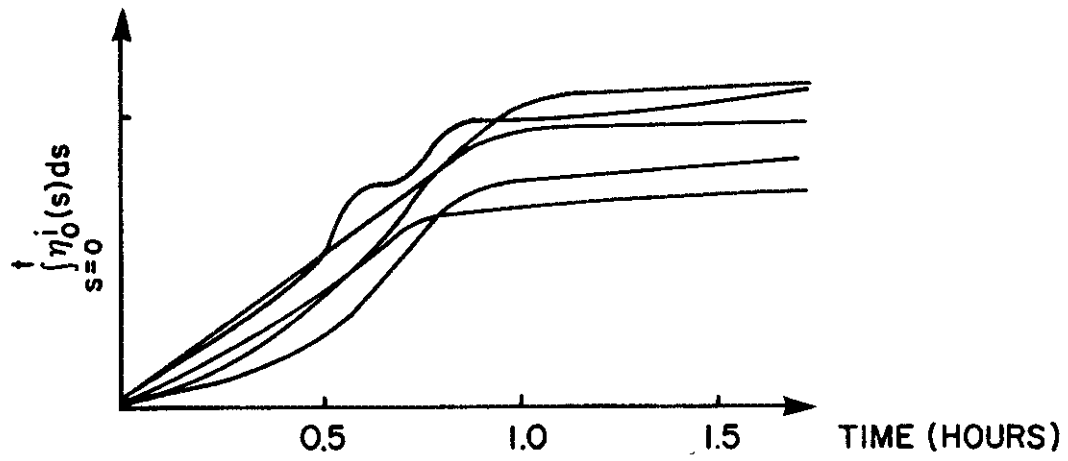

Fig. 11. Correlation Distributions $\eta_o^i(s)$, in Correlating $Q_g^i(t)$ and $e_g^i(t)$ for the Application Problem, Plotted in Summation (Distribution) Graph Form

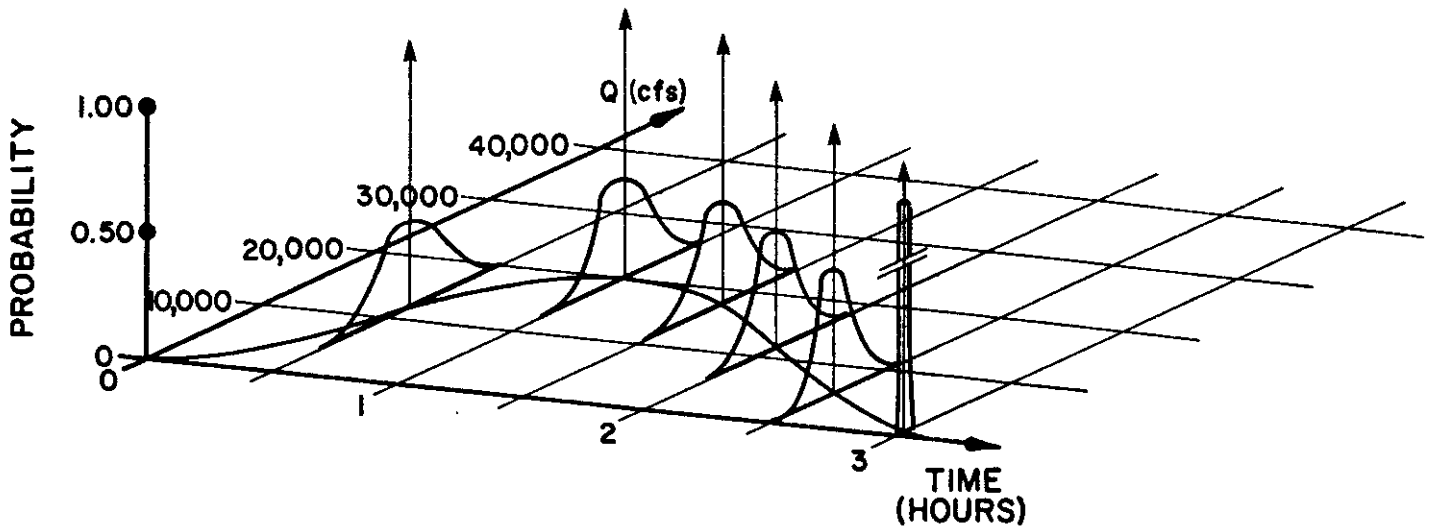

Fig. 12. The Hydrologic Model Distribution for a Predicted Response, $[Q_D(t)]$, from Input, $e_g^D(t)$. Heavy line is the Expected Distribution, $E[Q_D(t)]$.

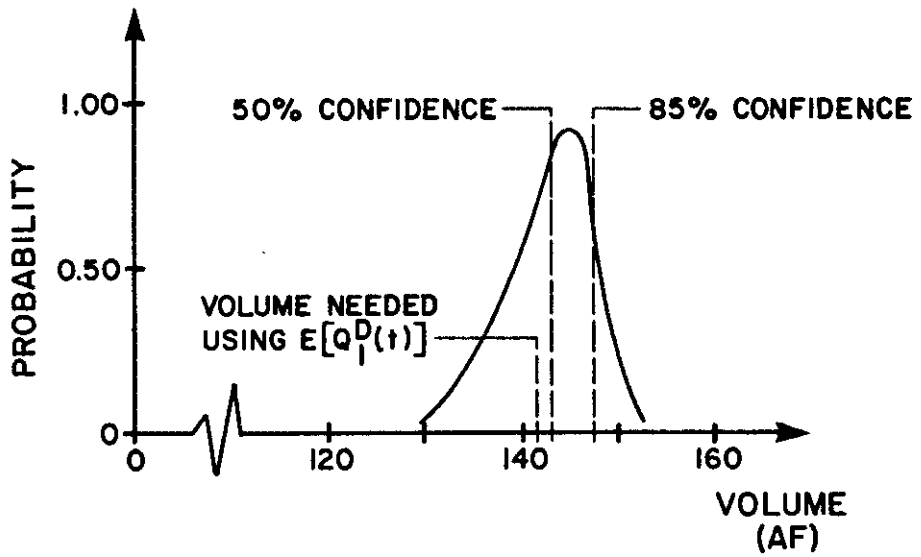

Fig. 13. Detention Basin Volume Requirements